Time-dependence of Heterogeneous Ice Nucleation by Ambient Aerosols: Laboratory Observations and a Formulation for Models

Jonas Jakobsson[1] (JJ), Vaughan T. J. Phillips[2]* (VTJP), and Thomas Bjerring-Kristensen[1] (TBK)

[1] Division of Nuclear Physics, Department of Physics, Lund University, Lund, Sweden
[2] Department of Physical Geography and Ecosystem Science (INES), Lund University, Lund, Sweden

Correspondence to: Vaughan Phillips (Vaughan.phillips@nateko.lu.se)

Abstract. The time dependence of ice-nucleating particle (INP) activity is known to exist, yet for simplicity it is often omitted in atmospheric models as an approximation. Hitherto only limited experimental work has been done to quantify this time dependency, for which published data are especially scarce regarding ambient aerosol samples and longer time scales.

In this study, the time dependence of INP activity is quantified experimentally for ambient environmental samples. The experimental approach includes a series of hybrid experiments with alternating constant cooling and isothermal experiments using a recently developed cold-stage setup called the Lund University Cold-Stage (LUCS). This approach of observing ambient aerosol samples provides the optimum realism for representing their time dependence in any model. Six ambient aerosol samples were collected representing aerosol conditions likely influenced by these types of INPs: marine, mineral dust, continental pristine, continental polluted, combustion-related and rural continental aerosol.

Active INP concentrations were seen to be augmented by about 40% to 100% (or 70% to 200%), depending on the sample, over 2 (or 10) hours. This degree of time dependence observed was comparable to that seen in previous published works. Our observations show that the minority of active ice nuclei (IN) with strong time dependency on hourly time scales display only weak time dependence on short time scales of a few minutes. A general tendency was observed for the natural time scale of the freezing to dilate increasingly with time. The fractional freezing rate was observed to steadily declines exponentially with the order of magnitude (logarithm) of the time since the start of isothermal conditions. A representation of time dependence for incorporation into schemes of heterogeneous ice nucleation that currently omit time dependence is proposed.

1 Introduction

The presence of ice nucleating particles (INPs) has been shown to influence cloud formation and cloud properties, precipitation
30   and thereby both local and global weather systems and climate (Phillips *et al.* 2003; Gettelmann *et al.* 2012; Kudzotsa 2014; Storelvmo 2017; Phillips and Patade 2021). Even though INPs have been studied for many decades, some aspects of their influence are still not fully understood (DeMott *et al.* 2011). One aspect where much uncertainty remains is the relevance of time in atmospheric ice processes.

35   According to the Intergovernmental Panel of Climate Change (Stocker *et al.* 2013) much of the uncertainty in projections of climate change by current global models are associated with the effects of atmospheric particles and aerosol-cloud-radiation interactions, and recent reviews indicate that a large degree of uncertainty prevails (Bellouin *et al.* 2020; Sherwood *et al.* 2020). The mechanisms for aerosol interaction with cold clouds have been explored with cloud models and are complex (Kudzotsa *et al.* 2016), as is also true globally (Storelvmo 2017).

An emerging area of interest is ice initiation for which there are many possible pathways (Cantrell and Heymsfield 2005; Phillips *et al.* 2007, 2020). At any given moment, only a small fraction of all condensed water in the atmosphere resides in the form of ice crystals. However, this small fraction has a disproportionately large impact on global precipitation which is mostly associated with the ice phase (Field and Heymsfield 2015). Homogeneous freezing of cloud droplets in the atmosphere
45   normally occurs at about -37 °C (Heymsfield *et al.* 2005), but heterogeneous freezing can occur at much warmer temperatures in the presence of rare, usually solid, aerosol particles that catalyse ice formation, termed ice nucleating particles (INPs). The presence of INPs has been shown to influence cloud formation and cloud properties (Phillips *et al.* 2003; Cantrell and Heymsfield 2005; Boucher *et al.* 2013; Kudzotsa 2014; Kudzotsa *et al.* 2016), precipitation (Lau and Wu 2003; Lohmann and Feichter 2005) and thereby both local and global weather systems and climate (Murray *et al.* 2012; Schill *et al.* 2020a,b;
50   Sanchez-Marroquin *et al.* 2020). INPs can be influential since they initiate crystals that can grow to become snow and graupel, which may melt, forming the '*ice crystal process*' of precipitation production (Rogers and Yau 1989).

The first ice in any mixed phase cloud is from activation of INPs. These have variable chemical composition, concentrations and activities in nature (Knopf *et al.* 2021). Mineral dust particles (e.g. from deserts) and soil dust particles may efficiently act
55   as INPs of relevance to mixed-phase clouds (e.g. Kanji *et al.*, 2017). A range of primary biological aerosol particles (PBAPs) such as e.g. bacteria, viruses, marine exudates, phytoplankton, fungal spores, pollen, lichen and plant fragments may facilitate immersion freezing potentially at relatively high temperatures (e.g. Kanji *et al.*, 2017). It is less clear to what extent combustion emissions, for example soot particles, may play a role as INPs in mixed-phase clouds (e.g. Kanji *et al.*, 2017).

60   For some thin wave clouds without precipitation, the observed number concentration of ice crystals is similar to that of active ice nuclei in the cloud (Eidhammer *et al.* 2010). Clearly, in such cold clouds, the chemistry and loading of INPs in the environment must affect the cloud properties. More generally there are many other potentially more prolific mechanisms for ice initiation (Cantrell and Heymsfield 2005; Field *et al.* 2017). Anyway, it is beneficial to simulate the first ice in mixed phase clouds accurately if detailed models are to represent the subsequent ice-microphysical processes adequately.

65

There exists a paradox in observations of natural mixed-phase stratiform glaciated clouds. Westbrook and Illingworth (2013) observed that ice precipitation from such a thin layer-cloud (mixed-phase from -12 to -13 °C) persisted for many hours and was produced by the ice crystal process. They argued qualitatively that this longevity could not be explained by mixing of environmental INPs into the layer cloud as the vertical motions were very weak and the cloud top level was constant, although

70   they did not quantify the turbulent fluxes of INP entrained from the environment. They hypothesised that time dependence of activity of ice nuclei (IN) was the cause. Despite in-cloud temperatures being isothermal, the stochastic nature of IN activity meant that a weak yet persistent long-term source of primary crystals would arise from this time dependence over times of many hours. However, their interpretation of the observations with this hypothesis has been contested by Ervens and Feingold (2013), who instead suggested the alternative explanation of in-cloud vertical motions and weak turbulence continually

75   activating INPs. The issue has not been resolved conclusively.

The first lab studies of time dependence of freezing began in the 1950s (reviewed by Pruppacher and Klett, 1997; 'PK97'). Two categories of models were proposed to explain the lab data, one with time dependence ('*the stochastic hypothesis*' that eventually became classical nucleation theory), (Bigg 1953ab) and one without time dependence ('*the singular hypothesis*',

80   sometimes referred to as '*the deterministic model*'), (Langham and Mason 1958). The singular hypothesis is an approximation and treats ice nucleation as a process occurring on active sites that become active instantaneously at distinct conditions that vary statistically among the INPs. An ice crystal is initiated immediately when an INP's characteristic conditions of freezing temperature and humidity are reached, as if it were a digital switch. This neglect of time dependence yields a simple dependence of primary ice initiation on thermodynamic vertical structure of the environment.

85

Classical or stochastic theory assumes that that embryonic ice clusters are continuously forming and disappearing (reviewed by PK97) at the interface of immersed aerosol particles. This is assumed to occur with a frequency that depends on the temperature. If an ice embryo reaches a critical size of stability, determined by the features of the surface, then ice is nucleated. Although modern lab observations have confirmed the existence of time dependence of IN activity, nevertheless the singular

90   hypothesis is still used in most cloud models owing to its validity as an approximation to the leading order behaviour of crystal initiation. Moreover, classical stochastic theory ('classical nucleation theory') can be difficult to represent because it is complex. In reality there is a probability distribution of efficiencies of active sites among INPs of any given aerosol species,

even for a population of identically sized particles (Marcolli *et al.* 2007). Classical nucleation theory can easily over-predict active INPs by orders of magnitude if such statistics are not properly considered.

95

In recent decades, laboratory experimental work to investigate time dependency of heterogeneous ice nucleation has been scarce. This is especially true for ambient environmental aerosols. Vali (1994) reported his earlier results for a small number of isothermal experiments (4 simple isothermal and 4 with a brief warming of the sample by 0.5 K or 1.3 K before the isothermal period) with an isothermal period of 10 to15 min on samples described as "*distilled water containing freezing nuclei*

100 *of unknown composition*", and isothermal temperatures between -16 and -21 °C. They concluded that the rate of freezing was dependent both on temperature and on time (see also Vali and Stansbury 1966). Welti *et al.* (2012), investigated aerosolized kaolinite particles in the immersion mode with the Zürich Ice Nucleation Chamber (ZINC) and observed time dependence by altering the flowrate through the instrument. They concluded that immersion freezing is at least partly a stochastic phenomenon, and recommended that time dependence should be included in numerical calculations of the evolution of mixed-

105 phase clouds.

Wright and Petters (2013) did experiments with Arizona Test Dust (ATD) with a droplet freezing array for various cooling rates between 0.1 and 5 K/min. They also included data for a total of two isothermal experiments (13.3 and 15.9 hours respectively). They concluded that their results implied a limited effect from time dependence equivalent to a few degrees of

110 error in the freezing temperature of aqueous droplets. Equally, Budke and Koop (2014) performed experiments with the commercially available snow inducer, Snowmax®, which was derived from *Pseudomonas syringae*, in the Bielefeld Ice Nucleation ARraY (BINARY). The technology applied in the present study is similar to that of BINARY. Budke and Koop measured time dependency with experiments for cooling rates ranging between 0.1 and 10 K/min and were able to show a weak dependency on time for Snowmax®. Knopf *et al.* (2020) investigated time-dependent freezing of illite for up to 2 hours

115 and confirmed that classical nucleation theory applies.

None of these aforementioned studies investigated environmental aerosol. No experiments studied time periods longer than a few minutes, except for Vali (1994), Wright and Petters (2013) and Knopf *et al.* (2020). Only a limited degree of time dependency has been observed. For example, an enhancement by about 50% in numbers of active INPs during the initial 20

120 s for a frozen fraction of about half was measured by Welti *et al.* (2012). Yet Vali (1994) observed this 50% change after about 15 min. In view of such controversy about the extent of time dependence in ambient INPs, the aim of the current study is to use an experimental approach to quantify time dependency for ambient environmental samples and to suggest a way to represent it in atmospheric models.

125 Our rationale here is that the optimum approach is to study ambient aerosol sampled directly from the environment if the time dependence of IN activity in atmospheric clouds is to be understood. The empirical parametrization by Phillips *et al.* (2008,

2013) follows a similar approach by treating the dependency of active INPs on chemistry, size and loading of aerosol species in terms of field observations of the background troposphere. Studying ambient aerosol samples provides the optimum representativeness of the aerosols observed, conferring realism on the cloud models that use the inferred schemes. On the other
130 hand, there is an inevitable cost from lack of identification of the precise chemical species initiating the ice in observed samples.

2 Method

2.1 Overview

There were three major stages to the experimental work performed in this study. Firstly, aerosol samples were collected for a period of about a year (from 2020-02-28) at the Hyltemossa research station, which is located in southern Sweden. Background
135 aerosol data was also collected at the research station during this period.

Secondly, the collected data were analysed to identify candidate samples that could be assumed to be likely dominated by, or at least possibly influenced by, aerosol particles representing six broadly defined aerosol classes:

- Marine dominated aerosol
140 - Mineral dust influenced aerosol
- Continental pristine aerosol
- Continental polluted aerosol
- Combustion dominated aerosol
- Rural continental aerosol

145

Thirdly these candidate samples were analysed with respect to ice nucleation activity with a combination of experiments for both continuous cooling rates and isothermal experiments for more than 10 hours.

The experimental setup enables automated control of the evolution over time of temperature of the freezing array for many
150 hours (> 10) with minimal risk of contamination. As noted below, any sample may be exposed to repeated freezing experiments with high precision (Sec. 2.3). This enables fresh questions to be addressed about time dependence of ice nucleation in natural clouds.

2.2 Selection/characterization of samples

155 **2.2.1 Sample collection**

Ambient air samples were collected at the Hyltemossa research station in southern Sweden (56°06'00"N 13°25'00"E). Hyltemossa is located in a forested area, and it is part of the ACTRIS network. Daily air samples were collected with a continuous sequential filter sampler (model SEQ47/50-RV, Sven Leckel Ingenieurbüro GmbH, Berlin, Germany) with a PM_{10} inlet and a flowrate of 1 m^3/h. The samples were collected on 47 mm polycarbonate track-etched membrane filters with 0.4

160 µm pore size. The sampling was set to 24-hour sampling for each filter and filter change was initiated at midnight. Because of the high pressure drop over the membrane filters not all filters were able to achieve a full 24-hour sampling. This issue unfortunately limited the selection of available samples, but the sampling coverage was deemed sufficient for this study. Filters were retrieved from the field station every 1-2 weeks, placed in sterile petrislide filter cassettes and stored at a temperature of about -20°C until analysis. Field blank samples were collected and handled in a manner identical to that for the sampled filters.

165

2.2.2 Sample classification according to likely dominant composition of INPs

Many aerosol samples were collected as noted above (Sec. 2.2.1). These were classified into six basic aerosol types as follows (section 2.1). In this study, we aimed at selecting samples likely to be dominated by different INP types at least of relevance to Northern Europe, and most likely of wider spatial-temporal relevance. In Table 1, we present supportive aerosol data related

170 to the six selected samples. Black carbon (BC) concentrations were measured with an Aethalometer (Model AE33, Magee scientific, Ljubljana, Slovenia) at Hyltemossa. Concentrations of particulate matter with diameters below 1 (PM_1) and 10 µm (PM_{10}) respectively were measured with an optical particle counter (OPC) (model Fidas 200, Palas GmbH, Karlsruhe, Germany) at the nearby Hallahus site (56°04'25"N, 13°14'88"E). The measurements at Hallahus are part of the European Monitoring and Evaluation Programme (EMEP). In addition, air mass back trajectories were inferred with the online HYSPLIT

175 model and they are presented in Fig. 1.

The BC concentration spans about one order of magnitude from 0.04 to 0.4 µg/m^3 between the selected samples, and the BC level correlates with the PM_1 level between these samples. In southern Sweden, the main components contributing to the PM_{10}-PM_1 are typically sea salt and/or dust particles. The 'combustion dominated' sample was so labelled, due to elevated levels of

180 BC and relatively low levels of PM_{10}-PM_1 in the ambient air. It was sampled on Dec. 7th during the heating season over a relatively short time window (local midnight to about 6:30 am). Hence, a pronounced fraction of the sampled PM was likely to originate from residential biomass combustion from local and/or Eastern European areas, as indicated by the back trajectories (Fig. 1).

185 The 'continental polluted' sample appears similar to the 'combustion dominated' sample in terms of the BC, PM1 and back trajectories passing over Eastern Europe during the residential heating season in March. However, the PM_{10}-PM_1 level is significantly higher for the 'continental polluted' sample (7.8 versus 3.0 μg/m³). The PM_{10}-PM_1 time series (not shown) peaks in the local afternoon, and we speculate that it in part is associated with local soil dust. Hence, it is not entirely clear whether (soil) dust and/or potentially combustion emissions may dominate the INP population in that sample.

190

The 'marine' sample (Sec. 2.1) is characterised by relatively low levels of BC, air mass back trajectories from the Northern Atlantic, and a relatively high level of PM_{10}-PM_1 (7.1 μg/m³), which may be associated with coarse sea salt particles. However, we cannot rule out the presence of INPs from land-based sources in Ireland/Great Britain, Denmark or locally in southern Sweden. The 'continental pristine' sample (Sec. 2.1) is characterised by low levels of BC, PM_1 and PM_{10}, and the air mass

195 back trajectories indicate that the likely aerosol sources areas are the Baltic Sea and/or Finland. The 'rural continental' sample (Sec. 2.1) is characterised by low levels of BC, PM_1 and an intermediate level of PM_{10}-PM_1 (4.7 μg/m³). In light of the air mass back trajectories, the aerosol sources could be land-based in Denmark/Norway or marine.

There were only limited local aerosol measurements in February, 2021, due to instrumental break down. Nevertheless, we

200 consider the INP population in the sample from Feb. 23rd, 2021 likely to be dominated by Saharan dust for the following reasons. The online SKIRON dust forecast predicted elevated levels of Saharan dust to be present in the boundary layer in southern Sweden some days around Feb. 23rd. Several urban measurement stations in southern Sweden showed highly elevated levels of PM_{10} during those days (www.dagensluft.se), with a typical maximum on Feb. 23rd. This period was characterised by unusually warm temperatures in southern Sweden, and the transport of Saharan air masses was covered in most popular media.

205 Also, the modelled 120h air mass back trajectories originate in the Mediterranean Sea with Sahara as a potential source region.

To summarise with respect to the 'Mineral dust influenced sample', we only have indirect evidence of high levels of Saharan dust in that sample. However, we found this sample to be the most likely candidate with an INP population dominated by dust. Nevertheless, we cannot rule out alternative European sources contributing to INPs in that sample.

210

Although all six samples could be classified approximately by their airmass type of origin, there was an inevitable lack of certainty about the chemical identity of their active INP. This limitation was a consequence of our overall approach of sampling ambient populations of INP from the real atmosphere. The mineral dust influenced and rural continental samples might be expected to have been enriched in mineral dust and PBAPs respectively, in view of the back-trajectory analysis (Sec.

215 2), but this is not proven by physico-chemical analysis. The rural continental sample had passed over half the length of Norway and southern Scandinavia, although it may have originated previously near the Arctic Ocean.

2.2.3 Sample preparation

The sampled filters were cut and a half filter was placed in sterile cryogenic vials while the other half of the filter was refrozen

220 and stored. Two mL of ultra-pure water (18.2 MΩ, <3 ppb VOC) was added to the vials and the sample was shaken at highest effect for 3 minutes on a laboratory vibrating vortex shaker. All sample preparation and handling of sampled filters were done in an ultra-clean environment in a laminar airflow cabinet, and all pipetting of sample and water was done with sterile pipette tips, discarded after single use. Field blank samples were treated identically to the collected filter samples.

225 **2.3 Experimental apparatus for measuring the ice activity of the samples**

The freezing apparatus used to perform the experimental work in this study was designed using elements inspired from several previously described similar cold-stage setups (Wright and Petters 2013; Budke and Koop 2014) and was named the Lund University Cold-Stage (LUCS). A schematic overview of the freezing array and the LUCS system is shown in Figure 2. In LUCS one hundred 1 µL sample drops are dispersed on siliconized hydrophobic glass slides, mounted in a freezing assembly

230 on a 40 x 40 mm temperature-controlled stage, (here forth termed the cold-stage) and control system (model LTS120, Linkham Scientific, Tadworth, United Kingdom). The cold-stage works by means of the Peltier effect, is fitted with internal temperature sensor and control system is capable to provide cooling down to -40°C (±0.1K). The device can be programmed to apply cooling or heating rates from 0.1 – 10 K/min, including isothermal temperature holds for extended periods of time.

235 The freezing array used to hold the sample is a layered construction (Fig. 2, upper left panel I). It consists of 1: siliconized hydrophobic glass slides (HR3-217, Hampton research, Aliso Viejo, US) on which the sample drops are dispersed. As the slides are hydrophobic, the sample drops do not float out on the surface, but maintains a roughly spherical form. The slides were flushed with ultra-pure water before use, and discarded after each drop population. A silicon grid (2) was used to keep the drops separated on the glass slides, and sealed each sample drop in an individual cell between the slides and a polycarbonate

240 lid (3), minimizing interaction between the drops (i.e. by Wegener-Bergeron-Findeisen type transfer of vapour or seeding of neighbouring drops by ice-splintering, surface growth or frost halos). The drops were spread out in an approximate circle on the cold-stage to avoid the corners, where the temperature may be less precise during temperature ramps. The grid was laser cut from medical grade silicone. The assembly was centred and held on the stage by a polycarbonate holder/guide. The assembly and the stage were encased in a small environmental chamber (part of the LTS120 Linkham system) and the sample

245 was observed through a quartz glass window (Figure 2, panel I, 4). Figure 2 (panel II) also shows the sample mounted in the assembly on the cold-stage.

Figure 2 (panel III) shows a schematic overview of the full LUCS setup. The cold-stage with the mounted sample (A) is placed in a laminar airflow cabinet (B) to avoid any airborne contamination of the sample during preparation and handling. A camera

250   system (C) consisting of a digital SLR (Canon Eos 6D mk II, Canon, JP), fitted with a 150 mm macro lens (IRIX 150mm f:2.8 Macro 1:1, Irix, ROK) and a continuous circular light source (R300, FandV, Helmond, NL) is fixed over the viewing window and controlled by a computer (D). The camera captures images of the sample during the experiments. A 15 L cryogenic water circulator (E) (model DC-3015, Drawell International Technologies Limited, Shanghai, China) is connected to the temperature-controlled stage and provides a steady flow of 8.5°C cooling water for the cold-stage, acting as a heat sink. The

255   relatively large water circulator is an important element in the setup for maintaining the thermal performance and stability of the cold-stage over extended periods of time, such as during long isothermal experiments. The environmental chamber was continuously purged with a low flow of dry, clean nitrogen gas (F), and a steady flow of dry filtered air (G) is directed over the viewing window to avoid any problems with fogging that may obscure the imaging.

260   The camera system captured images of the cold-stage in intervals as different cooling programs were applied to the sample (as detailed below in sections 2.4.1 and 2.4.2). The ice spectra for the samples were inferred from the generated images by semi-supervised image analysis. An example of an image generated by LUCS, which was used as the input for automated analysis of imagery, is shown in Figure 3. This displays unfrozen and frozen sample drops. As seen in Figure 3, the reflection of the circular light source is clearly visible in the liquid phase droplets, but rapidly disappears at the onset of freezing. This

265   transformation was used to determine the freezing temperature and time for all sample drops from the recorded images.

2.4 Experimental design

The ice nucleation activity of the samples was measured on five drop populations from each sample consisting of 100 drops, each with a volume of 1 µL. There were six samples of ambient environmental aerosol material in total (Sec. 2.1), collected

270   and classified as noted above (Sec. 2.2). For each of these drop populations at least three 2-hour isothermal experiments and one longer (11-16 hours) isothermal experiment were performed. The number of 2-hour isothermal experiments on each drop population was dictated by practical reasons, and the longer isothermal experiments were performed overnight. Measurements with a constant cooling rate of 2K/min were performed before and after the isothermal experiments, and also between some of the isothermal experiments to assure that the freezing spectra remained unchanged during the experimental time for each drop

275   population. The cooling programs used are defined as follows.

2.4.1 Experiments with constant cooling rate

The cooling program used for the experiments at constant rate of cooling is illustrated in Figure 4 (left panel). The sample was dispersed on the cold-stage and initially cooled with a fast cooling rate (-8K/min) from room temperature to -5°C. The sample

280   was then held at -5°C for one minute to assure thermal stability before a constant cooling rate of -2K/min was applied to the sample until it was fully frozen.

2.4.2 Isothermal experiments

The cooling program used for the isothermal experiments is illustrated in Figure 4 (right panel). The sample was initially
cooled with a fast cooling rate (-8K/min) from room temperature to -5 °C. The sample was then held at -5°C for one minute
to assure thermal stability before a constant cooling rate of -2 K/min was applied to the sample until 1K warmer than the target
isothermal temperature, where the cooling rate was decreased to -1K/min to avoid "overshooting" the target temperature. When
the target temperature was reached, the sample was held at this temperature for a determined period of time, ranging from 2
hours to over 10 hours. When the isothermal phase had elapsed, a constant cooling rate of -2K/min was then applied to the
sample until it was fully frozen.

The target temperature was chosen based on the initial constant cooling rate experiments for each sample to correspond to a
temperature where about 20-30% of the sample was frozen at the onset of the isothermal phase. This resulted in an isothermal
temperature of -16°C for the 'continental polluted' sample and -14°C for all other samples in this study.

2.4.3 Quality control

The experiments with constant cooling rates performed before, between and after the isothermal experiments (Sec. 2.4.2) were
primarily included to ensure that the freezing spectra of the samples remained consistent during the experimental time. This
was effectively a check on both the consistency of performance of the LUCS apparatus and the stability of samples with respect
to repeated measurements.

It was seen that the constant cooling experiments remained consistent for all samples during the experimental time, although
statistical variations were observed between individual drop populations. In addition, measurements were also carried out with
field blank samples to assure that no significant freezing could be observed to rise from either the measurement apparatus, the
polycarbonate filters or the handling procedures at temperatures overlapping with the samples. Specifically, isothermal
experiments were also done with both ultra-clean water and field blank samples, and no freezing events were observed during
2-hour isothermal experiments at the target temperatures used in this study (-14°C and -16°C).

3 Results

3.1 Validation of repeatability and sample stability

3.1.1 Freezing spectra

Figure 5 shows the average INP concentrations for the different samples inferred from four different droplet populations per
315   sample and 5 cooling ramps per droplet population. The Fletcher parameterisation (Fletcher, 1962) is included for comparison.
It is noteworthy, that the combustion dominated aerosol and the dust dominated aerosol contain relatively high and almost
identical concentrations of INPs in the temperature range from -20 to -10°C.

The marine aerosol sample (Sec. 2.1) also contains relatively high concentrations of active INPs. This is particularly
320   pronounced in the high temperature range (-12 to -7°C) and that may be associated with biological particles (PBAP INPs), as
seen also to a lesser extent for the rural continental sample. The 'continental polluted' aerosol sample (Sec. 2.1) contained
significantly lower concentrations of INPs relative to the combustion dominated aerosol, even though those samples shared
many characteristics with a suspected higher concentration of dust in the 'continental polluted' aerosol. The rural continental
aerosol sample contained INP concentrations very similar to the 'continental polluted' aerosol. The 'continental pristine'
325   aerosol is characterised by a different slope, with relatively low INP concentration in the high temperature range, and relatively
high concentrations in the low temperature range.

Preliminary results from a wider range of samples from the Hyltemossa site indicates that the median INP concentrations are
comparable to the Fletcher parameterisation, and the samples included in the current study do in many respects represent
330   typical features of the INP spectra. It was not possible to identify the specific INPs causing the freezing of individual droplets
with the type of approach applied in the current study. However, we do consider it highly likely that the INP types between
the samples differ significantly and represent typical ambient conditions of relevance to Northern Europe and surroundings.
So as to assess the robustness of the experiments with respect to repeatability and sample stability over the total experimental
time (up to > 24 hours), identical experiments with a constant cooling rate (Sec. 2.4.1) and the same aerosol sample were done
335   at various intervals (Sec. 2.4.3). Such cooling-only experiments were always performed before and after the isothermal
experiments for all drop populations from each sample, and also between some of the isothermal experiments.

Figure 6 shows that for most samples the difference in freezing temperature (for any given drop population) during repeated
constant cooling rate experiments is about 0.5K between freezing events at different times for any given value of freezing
340   fraction. There was a total of about 24 hours of exposure to repeated cycles of heating and cooling. However, for mineral
dust influenced and combustion dominated samples there was somewhat more variation (up to 1K), indicating that a small
minority of the drops may have undergone slight alterations in the nucleating ability of their immersed INPs during the freezing
cycles. Most of the variability for any given sample was related to statistical variations in the number of active INPs among

different drop populations, where the largest variation between drop populations was also observed for the mineral dust
345   influenced and combustion dominated samples.

In summary, the instrumental precision, repeatability of our experiments on each drop population and the absence of any
measurement changing bias are confirmed by these experiments. Variations of freezing temperature are of an order of 0.3 K,
which is much less than the signal from time dependence reported below.

350

3.1.2 Repeatability of freezing for individual drops

All observed drops were indexed and tracked through all freezing cycles, during both the isothermal experiments (Sec. 2.4.2)
and the experiments with constant cooling rates (Sec. 2.4.1). It was found that most drops froze in a relatively narrow
temperature range during repeated experiments (as also seen in Figure 6). The average temperature of at least four constant
355   cooling experiments (Sec. 2.4.1) on each drop allowed determination of the average freezing temperature and standard
deviation for each individual drop. This temperature will henceforth be referred to as the 'normal freezing temperature' for the
drop. The median of the standard deviations for four freezing cycles on each drop was about 0.25-0.34 K for this normal
freezing temperature (Marine dominated = 0.34 K, Mineral dust influenced = 0.31 K, Continental pristine = 0.25 K, Continental
polluted = 0.31 K, Combustion dominated = 0.32 K and Rural continental = 0.26 K) for the various samples, which is consistent
360   with previous reported observations (Vali 2008).

In Figure 7 the normal freezing temperatures (± 1 standard deviation) are displayed for those drops that were also observed to
freeze during the isothermal experiments. As seen in Figure 7, a majority of these drops that froze during the isothermal
experiments had a normal freezing temperature lower than the isothermal temperature for the experiments (marked in the
365   figure by the dotted cyan line). The difference for most drops displayed is about 1-2 K. The practically sigmoidal-like
distribution of normal freezing temperatures (Fig. 7) arises because the probability of any drop freezing during any isothermal
experiment decreases with decreasing normal freezing temperature below the isothermal temperature.

In summary, the effect from time-dependence of freezing over 2 hours is to raise the freezing temperature by mostly about 1-
370   2 K relative to the 'normal' value in cooling-only experiments.

3.2 Isothermal experiments

3.2.1 Isothermal time series and relaxation time

All examined samples showed the same general pattern during the isothermal phase (Sec. 2.4.2), with more abundant freezing
375 events occurring during the first minutes of the experiment and then a decreasing frequency of observed freezing events as
times increase (Fig. 8, blue dots). There was a significant variability between individual experiments and drop populations
from the same sample, but this should be expected both from the natural diversity of possible INPs in environmental samples
and the stochastic nature of ice activation.

380 Additionally, the data in the time series of freezing fraction were binned in logarithmically spaced time intervals and the
average freezing fraction was plotted for each bin (Fig. 8, yellow points). Figure 9 shows the relative enhancement of IN
activity during the entire 10-hour period of the isothermal phase (from final and initial averages of freezing fraction). The
corresponding enhancement over the first 2 hours is shown in Table 4. The two samples with the most enhancement are the
mineral dust influenced and rural continental samples, whereas the two with the least enhancement are continental pristine and
385 combustion dominated samples (Fig. 9).

Figure 10 shows the same averaged freezing fractions in terms of the fractional rate of freezing, $N_{ice}(t)^{-1} d\left(N_{ice}(t)\right)/dt$.
The fractional freezing rate has the same order of magnitude among all samples for any given time. The fractional rate
decreases almost exponentially with time since the start of the isothermal phase. This fractional rate must vary inversely with
390 the natural time scale of the freezing. This is explicable in terms of the more active INPs nucleating faster on shorter time
scales such that progressively less active and slower IN remain as the isothermal experiment progresses.

The limited literature of observations show that the unfrozen fraction is often seen to decay exponentially with time (Bigg
1953ab, Vali 1994, PK97; Knopf et al. 2020). Consequently, from our isothermal measurements the time dependency effects
395 were inferred by fitting the observations with this empirical model:

$$N_{ice}(t) = N_{ice,0} + \Delta N_{ice,\infty}\left(1 - e^{-\frac{t}{\tau}}\right) \tag{1}$$

In this model $N_{ice}(t)$ is the frozen fraction observed after time t since the start of the isothermal phase. Also, $N_{ice,0}$ is the
400 average initial ice fraction for the sample at the beginning of the isothermal phase, while $\Delta N_{ice,\infty}$ is the eventual increase of
ice fraction during the entire period of the isothermal phase. Here τ is a relaxation time.

A novel feature of our model (Eq (1)) is that the relaxation time-scale is allowed to evolve somehow over time ($\tau = \tau(t)$). Numerically, $\tau(t)$ can be determined from our empirical data by re-arranging Eq (1):

405

$$\tau(t) = -\frac{t}{\ln\left(1 - \frac{N_{ice}(t) - N_{ice,0}}{\Delta N_{ice,\infty}}\right)} \qquad (2)$$

The fitting of Eq (1) to the measurements was done as follows. First, $N_{ice,0}$ and $\Delta N_{ice,\infty}$ were estimated from the initial and final averages of freezing fraction during the isothermal phase (Fig. 8, initial and final yellow points). During the isothermal

410   period, from each average of the measured freezing fraction ($N_{ice}(t)$; yellow dots in Fig. 8) the relaxation time was inferred using Eq (2), as shown in Figure 11 (blue dots).

These inferred values of τ were seen to conform to a power law, as shown in Figure 11 (red lines):

415   $$\hat{\tau}(t) = C_i t^\alpha \qquad (3)$$

Note that both in the data and in the fits, as $t \to 0$ always $\hat{\tau}$ decreases (Fig. 11). Also, $\hat{\tau}$ increases monotonically with time throughout each isothermal period. This dilation of the relaxation time-scale with the age of exposure to constant conditions of temperature and humidity is explicable in terms of a statistical distribution of active sites among all the INPs. The most

420   active sites nucleate ice on shorter time-scales and are then 'lost', so the less active sites remain and they activate on longer time-scales, as time progresses.

The values for the fit parameters of Eq (3) are given in Table 2. With these, $N_{ice}(t)$ was reconstructed by applying the empirically fitted relaxation time, $\hat{\tau}(t)$ from Eq (3) for τ in Eq (1). Figure 8 (red lines) confirms that this empirical model

425   agrees with the experimental data used in its design.

In summary, the observed isothermal dependence on time of freezing conforms with a simple law of a freezing fraction increasing exponentially initially and then approaching an asymptotic value after an extended time of a few hours. The relaxation time increasingly dilates as time progresses throughout the isothermal phase, as expected from the most active INPs

430   being steadily depleted and leaving the less active INPs with longer characteristic times for activation.

3.2.2 Time dependent temperature shift for use in empirical parametrization of IN activity

Several IN parametrizations are based on observations involving a short time of exposure to constant conditions of humidity and temperature (e.g. about 10 s for a typical continuous flow diffusion chamber), (DeMott *et al*. 2015, Phillips *et al.* 2008,

435 2013). In order to modify such schemes so as to represent the time dependency of IN activity, we propose a temperature shift approach (see also Wright and Petters 2013). The modified active INP concentration, after exposure on longer time scales, may be assumed to equal the value from such a scheme for a shifted value of the temperature input, with the shift evolving over time ($\Delta T_X = \Delta T_X(t) \leq 0$).

440
$$n_{IN,X}(T, S_i, \Omega_X, t) = n_{IN,X*}(T + \Delta T_X(t, \dots), S_i, \Omega_X, t) \qquad (4)$$

Here, $n_{IN,X}$, is the active INP concentration (number per unit mass of air) as a function of time and of the ambient temperature T, the saturation of vapor with regard to ice, S_i and the available surface area , Ω_X, of aerosols of the X-th IN species. Also $n_{IN,X*}$ is the corresponding concentration from the original scheme without any time-dependence. Eq (4) here is based on our
445 empirical parameterization (EP) of heterogeneous ice nucleation by multiple species of aerosol (Phillips et al. 2008, 2013). Yet the same method is generally applicable to any other IN scheme that neglects time-dependency.

Figure 12 (blue dots) shows the temperature shift inferred for every measurement of freezing fraction (Fig. 8, blue dots) for all samples during the isothermal phase. This was done by averaging the freezing fraction over the first 10 s and matching this
450 with the prediction of the scheme by adjusting the constant of a proportionality between freezing fraction and $n_{IN,X*}$ for $t = 0$. So, by definition, $\Delta T_X = 0$ initially. Then at all times subsequently ΔT_X is numerically solved to satisfy Eq (4).

The shift values for the ambient temperature input to the IN scheme (EP) were seen to conform to a power law, as shown in Figure 12 (red dotted line):
455
$$\Delta T_X(t) = -A_i t^\beta \leq 0 \qquad (5)$$

All samples show a temperature shift of about 3 K and 5 K over the initial 2 and 10 hours respectively. Here t is the time since the start of isothermal conditions. Such an ambient temperature shift (downward) may be viewed as equivalent to a
460 corresponding opposite shift (upward), of comparable absolute magnitude, in characteristic freezing temperatures of most INPs.

3.3 Constant cooling rates with and without an isothermal phase

Figure 13 (drop populations: cyan lines; averaged for all drops: blue line) shows the freezing fraction as a function of
465 temperature during cooling at a constant rate (2 K/min) from -5°C until all samples are fully frozen, in namely the cooling-only experiments. As noted above for the same data displayed in Figure 6 (various colours), the freezing fraction goes from

almost zero to unity between about -10 and -20 °C. The temperatures for the freezing fraction of 0.5 are -14.8, -16.3, -14.5, -16.6, -15.8 and -17.8 °C for the marine, mineral dust influenced, continental pristine, continental polluted, combustion dominated and rural continental samples.

470

So as to reveal the influence from time-dependence, other experiments were performed interspersing constant cooling (2 K/min) with an isothermal phase (2 hours) as shown in Figure 13 (drop populations: magenta lines; averaged for all drops: red line), ('hybrid cooling-isothermal' experiments). Before the isothermal temperature was reached, for each sample the freezing fraction evolved identically for these hybrid cooling-isothermal experiments (red line) as for the ordinary cooling-only

475   experiments with a constant cooling rate (blue line). This indicates that the isothermal phase is reached with no "overshooting" of the target temperature, and that the lower cooling rate used for the last 1K does not influence the result.

Comparison of these hybrid cooling-isothermal experiments (red line) with the corresponding cooling-only experiments (blue line), subsequently after the isothermal temperature is reached, is a measure of the extent of time dependence for the samples

480   (Fig. 13). Hypothetically, if there were no time dependence (with each IN functioning as a perfect 'switch' with activation exactly at its characteristic freezing temperature), then the red line would simply follow the blue line, and the blue line would be relatively unchanged. The deviation of the red line from the blue line is a measure of time dependence arising from an extra 2 hours of exposure to constant conditions of temperature.

485   The eventual impact from time-dependence of freezing after 2 hours is evinced by the maximum difference in freezing temperature, between the red and blue lines, being about 1.6, 1.4, 0.7, 1.1 ,1.0 and 1.2K for the marine dominated, mineral dust influenced, continental pristine, continental polluted, combustion dominated and rural continental samples respectively. This is consistent with Fig. 9, which shows the total fractional increase in IN activity after 2 hrs of exposure to constant conditions. Thus, Figures 9 and 13 are consistent about which samples are the most (e.g. mineral dust influenced) or least (e.g.

490   continental pristine) time dependent.

Even after the end of the isothermal phase for some experiments, a deviation persists between the red and blue curves in Fig. 13. Some of the INPs, which normally would have activated at temperatures a few K colder than the isothermal temperature in the cooling-only experiment, actually activated at this temperature during the prolonged isothermal phase of the hybrid

495   experiment. Generally, as the temperature cools after the end of the isothermal phase, the hybrid experiment shows a freezing fraction that becomes increasingly similar to the cooling only experiment, as expected from the strong dependency on temperature of IN activity.

In summary, the observed time-dependence of freezing involves an upward shift in freezing temperature that increases with

500   time, by about 1-2 K after 2 hours for most drops. This further justifies the approach taken above for incorporating the effect

of time by means of a time-evolving temperature shift for schemes of heterogeneous ice nucleation in cloud models (Sections 3.2.2, 5).

4 Discussion

505 The present study attempts to fill a gap in knowledge about the role of time in real-world atmospheric ice processes, and how its influence should best be represented. Several previous studies have aimed to provide both a theoretical understanding and empirical data (Vali 1994; Welti *et al*. 2012; Wright and Petters 2013; Budke and Koop 2014; Knopf et al. 2020) so as to represent time dependence more accurately in ice nucleation. However, much of the previous published work studied the effect on idealized systems, and on relatively short time scales. Such studies are invaluable for understanding the basic physics of

510 time dependence in ice nucleation, but may be challenging to apply for practical use in atmospheric modelling.

Pioneering aspects of the present study include the fact that the effects of time dependence on ambient environmental samples are measured. This is done for far longer time scales (many hours) than observed hitherto in other studies (many mins) and provides more realistic data which can be applied directly to modify IN schemes and cloud models. It is, to the best of our

515 knowledge, the first study to date investigating time dependence on real-world ambient aerosol samples, although real precipitation samples were observed previously (e.g., Wright, 2014).

Generally, the results from the cooling-only experiments (e.g., Figure 6) show that the instrumental setup provides consistent measurements on each individual drop population for all samples, agreeing well before and during, as well as after, the repeated

520 isothermal experiments (Sec. 3.1.1). Together they comprise a total experimental time of up to 24 hours on each drop population. This shows that the measurements are robust, and that the samples do not change significantly during the instrumental time.

The data derived from the isothermal experiments (Figures 8 and 12) show much variability, which may be expected both

525 because of the stochastic nature of time dependence and from statistical variations in the composition of IN among different drop populations. However, when all freezing fraction data were averaged for a given sample and then fitted by Eq (1), the assumed fit was found to conform to the data (e.g., compare red curve and yellow points in Figure 8). Thus the approach with several repeated isothermal measurements on several drop populations from each sample is likely to give a realistic, albeit approximate, estimate of the effect of time dependence for the different samples. In short, the measurement datasets are

530 sufficient for adequate statistics to describe each sample.

Generally, in such lab measurements of freezing, an effect related to the composition of INPs, which may be a cause of uncertainty, is the risk of 'saturation' of active IN in the sample solution. As all samples in this study are environmental samples, there is a risk that multiple IN particles may be present in each sample drop, and the first IN to activate in any drop

535 will be the one represented in the results. For instance, if a drop contains a PBAP INP that nucleates ice at relatively high temperatures, this particle may obscure the presence of other INP in the same drop that would otherwise become active to cause freezing at lower temperatures or after longer times.

However, at the isothermal temperatures used in this study (-14 °C and -16 °C) the cumulative active INP concentrations for

540 the samples were estimated from their freezing spectra (Figure 5) and are of the order of 0.1 to 1 IN L^{-1} of air. This would imply that the number of active IN in each 1 µL sample drop should be less than unity (order of 0.1 to 1 per drop). That in turn confirms the applicability of the drop-freezing measurements for estimation of the atmospheric ice nucleating ability of our samples.

545 Curiously, as seen in Figure 7 for the rural continental sample, it indeed seems as if the overall active INP concentration is low, and that there may be multiple IN types in the same sample. One IN type activates close to the isothermal temperature; another IN type is less prevalent and activates about 5 K lower than the isothermal temperature. This is consistent with the observation that this sample, overall low in IN, may show a mode IN activating at warmer temperatures (e.g., possibly PBAPs or mineral dust). It should also be noted that in nature, even though a cloud drop generally originates from a single cloud

550 condensation nucleus (CCN), it is not unlikely that after some time several aerosol particles are present in cloud drops as a result of coagulation, particle scavenging and other processes. Thus the samples in this study may be representative of the aerosols studied in that sense.

5 Implementation of Time dependence Results in Cloud Models

555 In nature, there are many types of INPs that can be classified as belonging to broader aerosol groups frequently referred to as atmospherically relevant (Kanji *et al*. 2017), as used in some IN schemes (DeMott 2015; Phillips 2008, 2013). However, in the present project the samples investigated are from the ambient environment and must be assumed to contain a complex composition, where multiple INP species are abundant. Compared to opting for more well-defined artificial samples (e.g. Arizona test dust, Snowmax®) as done in some past studies (Welti *et al*. 2012; Budke *et al*. 2014), the approach of sampling

560 aerosols from the real troposphere entails several challenges (sections 1 and 2.2). In particular, the identity of the INPs dominating the ice initiation in each of our samples is uncertain.

Nevertheless, the time dependence of the temperature shift that we observed (section 3.2) allows preliminary representation of time dependence of IN activity in atmospheric models. Comparison between cooling-only and hybrid cooling-isothermal

565 experiments further illustrates how that the effects from time-dependence may be expressed in terms of a shift in freezing temperature that increases with time (Sec. 3.3).

Eq (5) can be applied in any cloud model to modify such IN schemes for inclusion of time dependence (Table 3), (Sec. 3.2.2). There are several obstacles to overcome regarding implementation of our observed temperature shift. First, there is the issue

570 of which of our samples is most likely to represent each IN species in any model. From the classification of our samples (section 2.2) from the Hyltemossa field station, some likely correspondences may be hypothesized (e.g., perhaps the mineral dust influenced sample for dust IN; possibly the combustion-dominated sample for non-biological carbonaceous IN).

Secondly, there is the problem about how to define the time of exposure to constant conditions represented by t in Eq (5) when

575 it is applied in a model. In a natural cloud there are vertical motions as well as long-lived regions of little ascent. For practical implementation in a cloud model, we make the simplification that t in Eq (5) may be approximated by the time since the current parcel first entered the cloud. Thus, t may be estimated by a passive tracer, Q, that decays exponentially with time while in cold clouds ($T < 0$ °C). The passive tracer evolves as follows in the cloud model:

580
$$\frac{DQ}{Dt} = \begin{cases} \frac{Q}{\tau_Q} & \text{while in cold clouds} \\ 0 & \text{otherwise} \end{cases} \tag{6}$$

Outside of cold clouds $Q = 1$ everywhere. From the solution, $Q = \exp(-t/\tau_Q)$, the time since entering the cold clouds, t, may be inferred from the local predicted value of Q. This is then used in Eq(5) to get the temperature shift $\Delta T(t)$ for species X, for the classification assumed above, which then in turn is added to the temperature input for the IN scheme.

585

Finally, if very long-lived clouds are being simulated, we recommend applying Eq (5) beyond $t = 10$ hours, providing $\Delta T < 10$K and thresholding at 10K otherwise. In view of the experimental limitations of our data, we make a simplification assumption that the temperature shift is independent of temperature but has a different functional form for each INP species. In summary, our lab observations with Eqs (4)-(6) provide a simple way to include time dependence in IN schemes commonly

590 applied in atmospheric models. This enables the glaciation of cold long-lived clouds to be simulated.

6 Conclusions

In the present study we present empirical data about the time dependence of heterogeneous ice nucleation for six ambient environmental aerosol samples. Ambient environmental samples, representing a variety of aerosol types expected to be

595   dominated by certain INP species, were investigated. As they were natural samples, they must be assumed to contain a complex composition, where multiple INP species may be active. Although this approach involves less certainty about the chemical identity of the active INPs observed, it yields results with maximum realism.

The conclusions were as follows:

600   1.   Clear effects from time dependency were observed on a level comparable to previous published works, with a percentage enhancement over 10 mins and 2 hours of about 20–40% and 40–100% respectively (Vali 1994; Welti *et al.* 2012; Wright and Petters 2013; Budke and Koop 2014). There was variation seen among the various samples. Time dependency effects were observed to be strongest for the rural continental and mineral dust influenced samples, and weakest for the continental pristine and combustion dominated samples.

605

2.   The repeatability of freezing of individual drops, selected from those that froze during the isothermal phase of the hybrid cooling-isothermal experiments, during the successive cycles of constant cooling (each being about 3 mins in duration for 5 K cooling), was mostly limited to about ± 0.3 K for the freezing temperature for all 6 samples. However, on the much longer time scale (2 hours) of the original isothermal phase about half of them had frozen at a freezing

610   temperature between 1 and 5 K warmer than for the constant cooling rate cycles. Thus, our observations show that the minority of active IN with strong time dependence on hourly time scales display only weak time dependence on short time scales of a few minutes.

3.   In the isothermal experiments, there was an enhancement of active INP concentrations by about 40% to 100% and by

615   about 70% to 200%, depending on the sample, over 2 and 10 hours respectively. The strongest time-dependence was seen for the mineral dust influenced and rural continental samples.

4.   There is a general tendency for the natural time scale of the freezing to dilate increasingly as time progresses during each isothermal experiment.

620   a.   The fractional freezing rate steadily declines exponentially with time. It decreases with an increasing order of magnitude (logarithm) of the time since the start of the isothermal phase. The fractional freezing rate may be viewed as the reciprocal of the time-scale of freezing.

     b.   A simple empirical law with an exponential time dependence, asymptotically approaching a maximum freezing fraction, is fitted to the average of all drop populations for any sample. This time dependence is

625   expressed in terms of the ratio of time to a natural relaxation time, which in term depends on time. This
          yields a simple power law dependence of the relaxation time on time itself, again with a steady dilation over
          time.

     5.   Comparison of cooling-only and hybrid cooling-isothermal experiments reveals that exposure to constant conditions
630   for long times causes an upward shift in freezing temperature that increases with time, by about 1-2 K after 2 hours
          for most drops. There is a wide variation in the extent of this shift among the individual drops in any drop population,
          following a sigmoidal-like statistical distribution.

     6.   A technique for representation of time dependence is proposed for incorporation into schemes of heterogeneous ice
635   nucleation that currently omit time dependence (e.g., Phillips *et al.* 2008, 2013; DeMott *et al.* 2015; Patade *et al.*
          2019, 2021), as are commonly used in cloud models (Eqs (4)-(6), Table 3, Sections 3.2.2 and 5). This involves a shift
          that depends on time for the ambient temperature input for these schemes when determining the active number of IN.
          Our observations reveal a simple power law dependence of this ambient temperature shift with time, reaching about
          3 K and 5 K of cooling over the initial 2 and 10 hours respectively.

640

In summary, the time dependence of IN activity of ambient aerosols sampled from the free troposphere is characterized. This
reveals a steady dilation of the natural time scale of freezing during exposure to constant conditions of temperature as the more
active INPs are depleted. A simple empirical approach is provided for IN schemes by introducing a time-dependent
temperature shift. This enables the glaciation and precipitation of cold long-lived clouds, observed in field campaigns (e.g.
645 Westbrook and Illingworth 2013), to be simulated.

7 Acknowledgements

The project was funded by a research grant to VTJP, from the Swedish Research Council for Sustainable Development
(''FORMAS'' Award 2018-01795). The topic of this award concerns the effects on clouds and climate arising from the time-
650 dependence of heterogeneous ice nucleation.   VTJP planned and directed the present study. Also, we thank the Royal
Physiographic Society of Lund, the Walter Gyllenberg Foundation, the Crafoord Foundation (grant 20190964) and the strategic
research area, MERGE, for financial support. The research leading to the supportive aerosol results from Hyltemossa have
received funding from the European Union's Horizon 2020 research and innovation programme under grant agreement No
654109. We acknowledge support from Patrik Nilsson, Marcin Jackowicz-Korczynski, Erik Ahlberg and Adam Kristensson
655 for support with filter sampling and operation of the Hyltemossa field station. We thank ACTRIS for support and access to
data. We thank the European Monitoring and Evaluation Programme (EMEP) for access to PM data.

8 Author Contributions

JJ carried out the experimental work with support from TBK. JJ did most of the data analysis with support from VTJP and
660 minor contributions from TBK. All authors were involved in the experimental design and the interpretation of results. JJ and
VTJP drafted the first manuscript version together, and all authors contributed to the manuscript writing.

9 Competing Interests

The authors declare that they have no conflict of interest.
665

References

Bellouin, N., Quaas, J., Gryspeerdt, E., Kinne, S., Stier, P., Watson-Parris, D., and co-authors, 2020: Bounding global aerosol radiative forcing of climate change. *Reviews of Geophysics*, **58**, e2019RG000660

670

Bigg, E. K., 1953a: The supercooling of water. *Proceedings of the Physical Society. Section B*, **66**(8), 688

Bigg, E. K., 1953b: The formation of atmospheric ice crystals by the freezing of droplets. *Q. J. R. Met. Soc.*, **79**(342), 510-519

675

Boucher, O., Randall, D., Artaxo, P., Bretherton, C., Feingold, G., Forster, P., and co-authors, 2013: *Clouds and aerosols.* In "Climate change 2013: the physical science basis. Contribution of Working Group I to the Fifth Assessment Report of the Intergovernmental Panel on Climate Change" (pp. 571-657). Cambridge University Press

680 Budke, C., and T. Koop, 2015: BINARY: an optical freezing array for assessing temperature and time dependence of heterogeneous ice nucleation. *Atmospheric Measurement Techniques*, **8**(2), 689-703

Cantrell, W., and A. Heymsfield, 2005: Production of ice in tropospheric clouds: A review. *Bull. Am. Meteorol. Soc.*, **86**(6), 795-808

685

DeMott, P. J., and co-authors, 2011: Resurgence in ice nuclei measurement research. *Bull. Am. Meteorol. Soc.,* **92,** 1623–1635

DeMott, P. J., Prenni, A. J., McMeeking, G. R., Sullivan, R. C., Petters, M. D., Tobo, Y., and co-authors, 2015: Integrating laboratory and field data to quantify the immersion freezing ice nucleation activity of mineral dust particles. *Atmospheric*
690 *Chemistry and Physics*, **15**(1), 393-409

Eidhammer, T., DeMott, P. J., Prenni, A. J., Petters, M. D., Twohy, C. H., Rogers, D. C., and co-authors, 2010: Ice initiation by aerosol particles: Measured and predicted ice nuclei concentrations versus measured ice crystal concentrations in an orographic wave cloud. *Journal of the atmospheric sciences*, **67**(8), 2417-2436

695

Ervens, B., and G. Feingold, 2013: Sensitivities of immersion freezing: Reconciling classical nucleation theory and deterministic expressions. *Geophysical Research Letters*, **40**(12), 3320-3324

Field, P., and co-authors, 2017: Secondary ice production: current state of the science and recommendations for the future.
700   *Met. Monogr.*, **58** (Chapter 7)**,** 7.1-7.19

Gettelman, A., X. Liu, D. Barahona, U. Lohmann, and C. Chen, 2012: Climate impacts of ice nucleation. *J. Geophys. Res.*,
117, D20201, doi:10.1029/2012JD017950

705   Kanji, Z. A., Ladino, L. A., Wex, H., Boose, Y., Burkert-Kohn, M., Cziczo, D. J., and M. Krämer, 2017: Overview of ice
nucleating particles. *Meteorological Monographs*, **58**, 1-1

Knopf, D. A., Alpert, P. A., Wang, B., and J. Y. Aller, 2011: Stimulation of ice nucleation by marine diatoms. *Nature
Geoscience*, **4**(2), 88-90

710

Knopf, D. A., P. A. Alpert, A. Zipori, N. Reicher, and Y. Rudich, 2020: Stochastic nucleation processes and substrate
abundance explain time-dependent freezing in supercooled droplets. *Clim. Atmos. Sci.*, **3,** 1-9

Knopf, D. A., K. R. Barry, T. A. Brubaker, L. G. Jahl, K. A., L. Jankowski, J. Li, Y. Lu, L. W. Monroe, K. A. Moore, F. A.
715   Rivera-Adorno, K. A. Sauceda, Y. Shi, J. M. Tomlin, H. S. K. Vepuri, P. Wang, N. N. Lata, E. J. T. Levin, J. M. Creamean,
T. C. J. Hill, S. China, P. A. Alpert, R. C. Moffet, N. Hiranuma, R. C. Sullivan, A. M. Fridlind, M. West, N. Riemer, A. Laskin,
P. J. DeMott, and X. Liu, 2021: Aerosol–ice formation closure: A Southern Great Plains field campaign. *Bull. Am. Met. Soc.,*
accepted.

720   Kudzotsa, I., 2014: *Mechanisms of aerosol indirect effects on glaciated clouds simulated numerically*. University of Leeds.

Kudzotsa, I., Phillips, V. T., and S. Dobbie, 2016: Aerosol indirect effects on glaciated clouds. Part 2: Sensitivity tests using
solute aerosols. *Quarterly Journal of the Royal Meteorological Society*, **142**(698), 1970-1981

725   Langham, E. J., and B. J. N. Mason, 1958: The heterogeneous and homogeneous nucleation of supercooled water. *Proceedings
of the Royal Society of London. Series A. Mathematical and Physical Sciences*, **247**(1251), 493-504

Lau, K. M., and H. T. Wu, 2003: Warm rain processes over tropical oceans and climate implications. *Geophysical Research
Letters*, **30**(24).

730

Lohmann, U., and J. Feichter, 2005: Global aerosol indirect effects: A review. *Atmos. Chem. Phys*, **5,** 715-737

Marcolli, C., Gedamke, S., Peter, T., and B. Zobrist, 2007: Efficiency of immersion mode ice nucleation on surrogates of mineral dust. *Atmospheric Chemistry and Physics*, **7**(19), 5081-5091

735

Morris, C. E., Conen, F., Alex Huffman, J., Phillips, V., Pöschl, U., and D. C. Sands, 2014: Bioprecipitation: a feedback cycle linking Earth history, ecosystem dynamics and land use through biological ice nucleators in the atmosphere. *Global change biology*, **20**(2), 341-351

740   Murray, B. J., O'Sullivan, D., Atkinson, J. D., and M. E. Webb, 2012: Ice nucleation by particles immersed in supercooled cloud droplets. *Chemical Society Reviews*, **41**(19), 6519-6554

Niedermeier, D., Ervens, B., Clauss, T., Voigtländer, J., Wex, H., Hartmann, S., and F. Stratmann, 2014: A computationally efficient description of heterogeneous freezing: A simplified version of the Soccer ball model. *Geophysical Research*
745   *Letters*, **41**(2), 736-741

Patade, S., Deshmukh, A., Dangat, P., Axisa, D., and co-authors, 2019: Role of liquid phase in the development of ice phase in monsoon clouds: Aircraft observations and numerical simulations. *Atmospheric Research*, **229**, 157-174

750   Patade, S., V. T. J. Phillips, P. Amato, H. G. Bingemer, S. M. Burrows, P. J. DeMott, F. L. T. Goncalves, D. A. Knopf, C. E. Morris, C. Alwmark, P. Artaxo, C. Pöhlker, J. Schrod, and B. Weber, 2021: Empirical formulation for multiple groups of primary biological ice nucleating particles from field observations over Amazonia. *J. Atmos. Sci.,* **78**, in press

Phillips, V. T. J., T. W. Choularton, A. J. Illingworth, R. J. Hogan, and P. R. Field, 2003: Simulations of the glaciation of a
755   frontal mixed-phase cloud with the Explicit Microphysics Model (EMM). *Q. J. R. Met. Soc.,* **129**, 1351-1371

Phillips, V. T., Donner, L. J., and S. T. Garner, 2007: Nucleation processes in deep convection simulated by a cloud-system-resolving model with double-moment bulk microphysics. *J. Atmos. Sci.*, **64**(3), 738-761

760   Phillips, V. T., DeMott, P. J., and C. Andronache, 2008: An empirical parameterization of heterogeneous ice nucleation for multiple chemical species of aerosol. *J. Atmos. Sci.*, **65**(9), 2757-2783

Phillips, V. T., Demott, P. J., Andronache, C., Pratt, K. A., Prather, K. A., Subramanian, R., and C. Twohy, 2013: Improvements to an empirical parameterization of heterogeneous ice nucleation and its comparison with observations. *J.*
765   *Atmos. Sci.*, **70**(2), 378-409

Phillips, V. T. J., and S. Patade, 2021: Multiple Environmental Influences on the Lightning of Cold-Based Continental Cumulonimbus Clouds. Part II: Sensitivity Tests and the Land- Ocean Contrast. *J. Atmos. Sci.*, in press

770   Pruppacher, H. and J. Klett, 1997: *Microphysics of clouds and precipitation*. Kluwer Academic Publishers.

Rogers, R. R., and M. K. Yau, 1989: *A short course in cloud physics.*   Pergamon Press

Sanchez-Marroquin, A., Arnalds, O., Baustian-Dorsi, K. J., Dagsson-Waldhauserova, P., Harrison, A. D., Maters, E. C., and
775   co-authors, 2020: Iceland is an episodic source of atmospheric ice-nucleating particles relevant for mixed-phase clouds. *Science advances*, **6**(26), eaba8137.

Schill, G. P., DeMott, P. J., Emerson, E. W., Rauker, A. M. C., Kodros, J. K., Suski, K. J., and co-authors, 2020a: The contribution of black carbon to global ice nucleating particle concentrations relevant to mixed-phase clouds. *Proceedings of*
780   *the National Academy of Sciences*, **117**(37), 22705-22711.

Schill, G. P., Froyd, K. D., Bian, H., Kupc, A., Williamson, C., Brock, C. A., and co-authors, 2020b: Widespread biomass burning smoke throughout the remote troposphere. *Nature Geoscience*, **13**(6), 422-427.

785   Stein, A. F., Draxler, R. R., Rolph, G. D., Stunder, B. J., Cohen, M. D., and F. Ngan, 2015: NOAA's HYSPLIT atmospheric transport and dispersion modeling system. *Bulletin of the American Meteorological Society*, **96**(12), 2059-2077

Stocker, T. F.; Qin, D.; Plattner, G.-K.; Alexander, L. V.; Allen, S. K.; Bindoff, N. L.; Bréon, F.-M.; Church, J. A.; Cubasch, U.; Emori, S.; Forster, P.; Friedlingstein, P.; Gillett, N.; Gregory, J. M.; Hartmann, D. L.; Jansen, E.; Kirtman, B.; Knutti, R.;
790   Kumar, K. K.; Lemke, P.; Marotzke, J.; Masson-Delmotte, V.; Meehl, G. A.; Mokhov, I. I.; Piao, S.; Ramaswamy, V.; Randall, D.; Rhein, M.; Rojas, M.; Sabine, C.; Shindell, D.; Talley, L. D.; Vaughan, D. G.; Xie, S.-P., 2013: *Technical Summary*. In Climate Change 2013: The Physical Science Basis. Contribution of Working Group I to the Fifth Assessment Report of the Intergovernmental Panel on Climate Change; Cambridge, UK and New York, NY, USA.

795   Storelvmo, T., 2017: Aerosol effects on climate via mixed-phase and ice clouds. *Annual Review of Earth and Planetary Sciences*, **45**, 199-222

Vali, G., and E. J. Stansbury, 1966: Time-dependent characteristics of the heterogeneous nucleation of ice. *Canadian Journal of Physics*, **44**(3), 477-502.
800

Vali, G., 1994: Freezing rate due to heterogeneous nucleation. *Journal of Atmospheric Sciences*, **51**(13), 1843-1856.

Welti, A., Lüönd, F., Kanji, Z. A., Stetzer, O., and U. Lohmann, 2012: Time dependence of immersion freezing: an experimental study on size selected kaolinite particles. Atmospheric Chemistry and Physics, **12**(20), 9893-9907

805

Westbrook, C. D., and A. J. Illingworth, 2013: The formation of ice in a long-lived supercooled layer cloud. *Quarterly Journal of the Royal Meteorological Society*, **139**(677), 2209-2221

Wright, T. P., and M. D. Petters, 2013: The role of time in heterogeneous freezing nucleation. *J. Geophys. Res. Atmos.*, **118**,
810   3731–3743, doi:10.1002/jgrd.50365.

Wright, T. P., 2014: Experimental Studies in Ice Nucleation. *Ph. D. Thesis.* North Carolina State University.

815

Figures
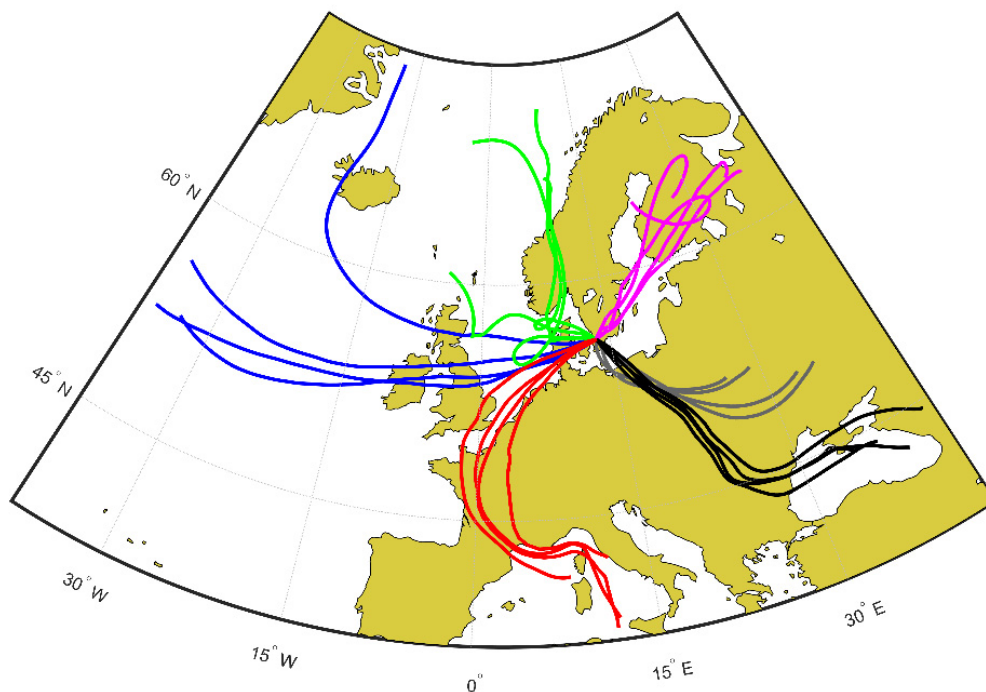
820   **Figure 1:** Back trajectories for the 6 aerosol samples, results from the HYSPLIT model (Stein et al. 2015). The displayed samples are marked in various colours (blue = Marine, red = Mineral dust influenced, magenta = Continental pristine, grey = Continental polluted, black = Combustion dominated and green = rural continental). The individual lines for each sample show back trajectories for the airmass arriving at the Hyltemossa station initiated every 6 hours during the sampling dates, 500 meters above ground level.

825
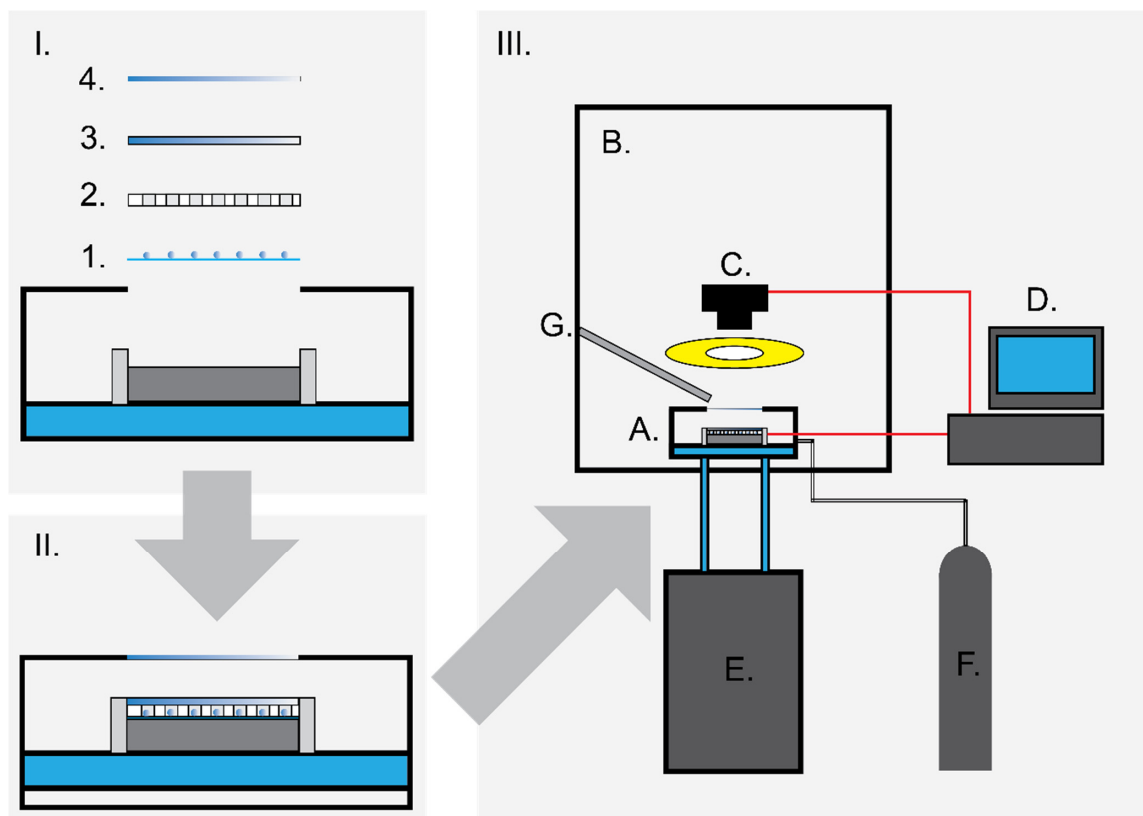
Figure 2: The Lund University Cold-stage (LUCS). **Upper left panel, I:** The freezing array design. The sample is placed on siliconized hydrophobic glass substrates (1) which are placed on the cold-stage. The sample drops are separated by a silicone grid (2) confining each drop to an individual cell, between the glass substrate and a polycarbonate lid (3). The freezing array is in turn encased in a small environmental chamber, with a quarts viewing window (4). **Lower left panel, II:** The sample mounted in the assembled freezing array. **Right panel, III:** Overview of the LUCS system. The cold-stage (A) is placed in a laminar airflow cabinet (B) to avoid any possible contamination. A camera system with a circular continuous LED light source is fixed above the cold-stage's viewing window and focused on the cold-stage. The camera is controlled by a computer (D), and a cryogenic water circulator (E) provides the cold-stage with 8.5 °C cooling water, acting as a heat sink for the device. The environmental chamber is continuously purged with dry nitrogen gas, and a flow of dry, HEPA-filtered air (G) is directed at the viewing window to eliminate potential fogging at low temperatures.

840
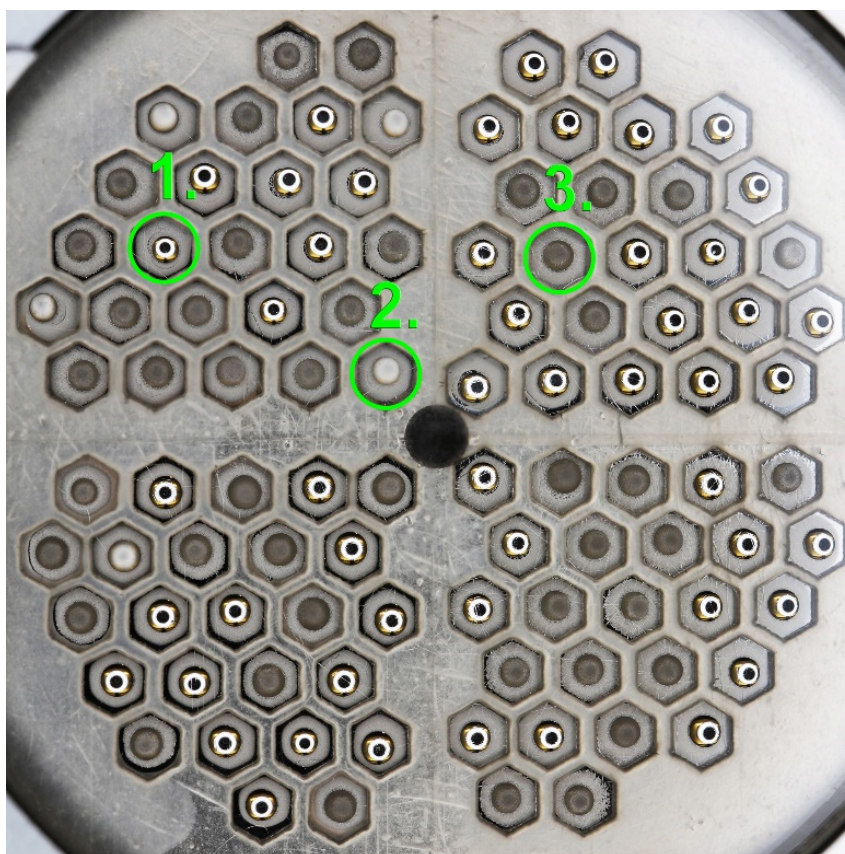
Figure 3: An image generated by LUCS, used as the input data to determine drop freezing events. The image shows the outlay
845   of the 100 sample drops on the 40 x 40 mm stage; each drop confined to a sealed cell. The image shows drops that are still in
the liquid phase and reflect the light from the circular light source (1), drops that are just undergoing freezing (2) and drops
that are fully frozen (3).

850
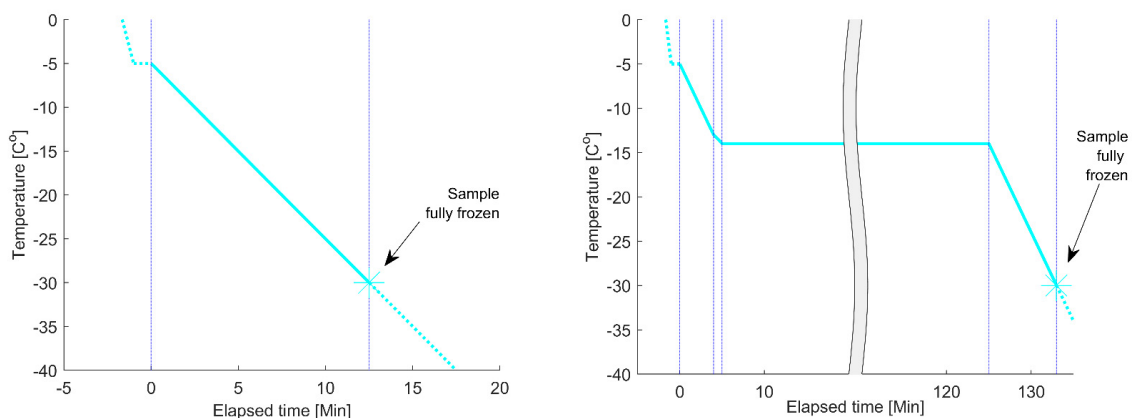
Figure 4: The cooling programs used in this study. The cyan lines display the evolution of temperature as a function of time, the blue dotted lines indicate where the cooling rate is changed and where the experiment is completed (when the sample is fully frozen). Left panel: the cooling program for the constant cooling rate experiments. Right panel: The cooling program

855 used for the 2-hour isothermal experiments. One isothermal experiment with a longer isothermal period (11 – 16 hours) was also done on each drop population (not shown). In this figure, the timescale starts (t = 0) at the first cooling ramp after the 1 min pause at -5 °C, all times referred to in the analysis for the isothermal experiments are from the start of the isothermal phase, if nothing else is specifically stated.

860
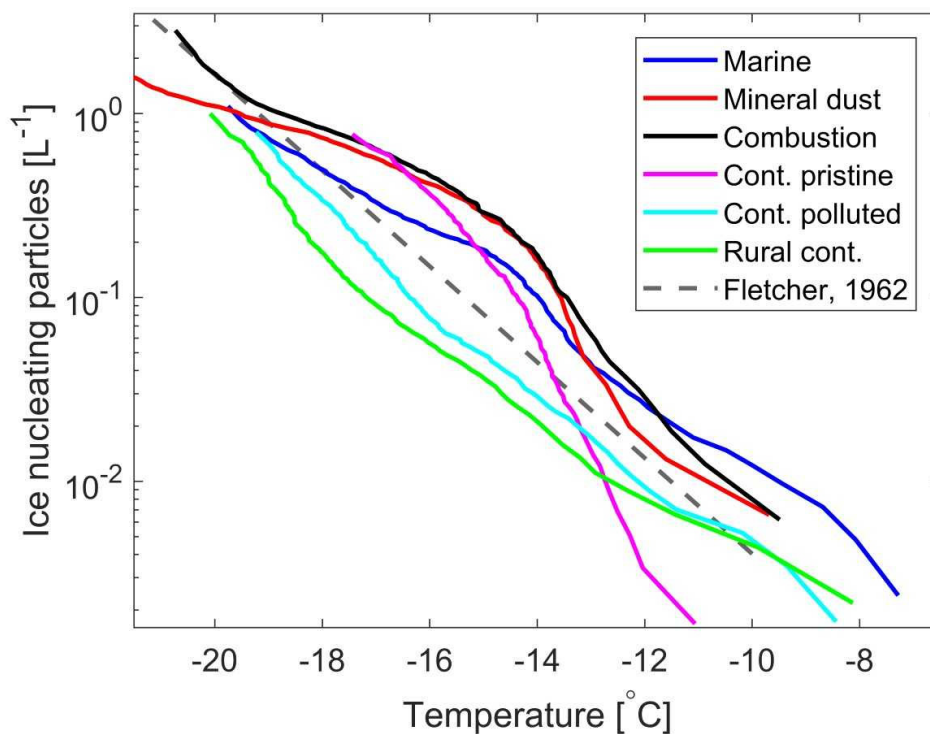
865 **Figure 5:** Ambient concentrations (per Litre of air) of ice nucleating particles versus temperature for the six samples of aerosol material studied (dark blue for the marine dominated sample, red for the mineral dust influenced sample, magenta for the continental pristine sample, cyan for the continental polluted sample, black for the combustion dominated sample and green for rural continental sample). The Fletcher (1962) parameterisation is included for comparison. The averaged INP spectra are based on five different droplet populations (in total 500 droplets, each 1 μL) per sample and at least 4 cooling ramps per droplet

870 population with a constant cooling rate (2 K/min). The reproducibility was generally very high for a given sample and a given droplet population. Variability was more pronounced in the high temperature range of the spectra, where fewer freezing incidents were observed.
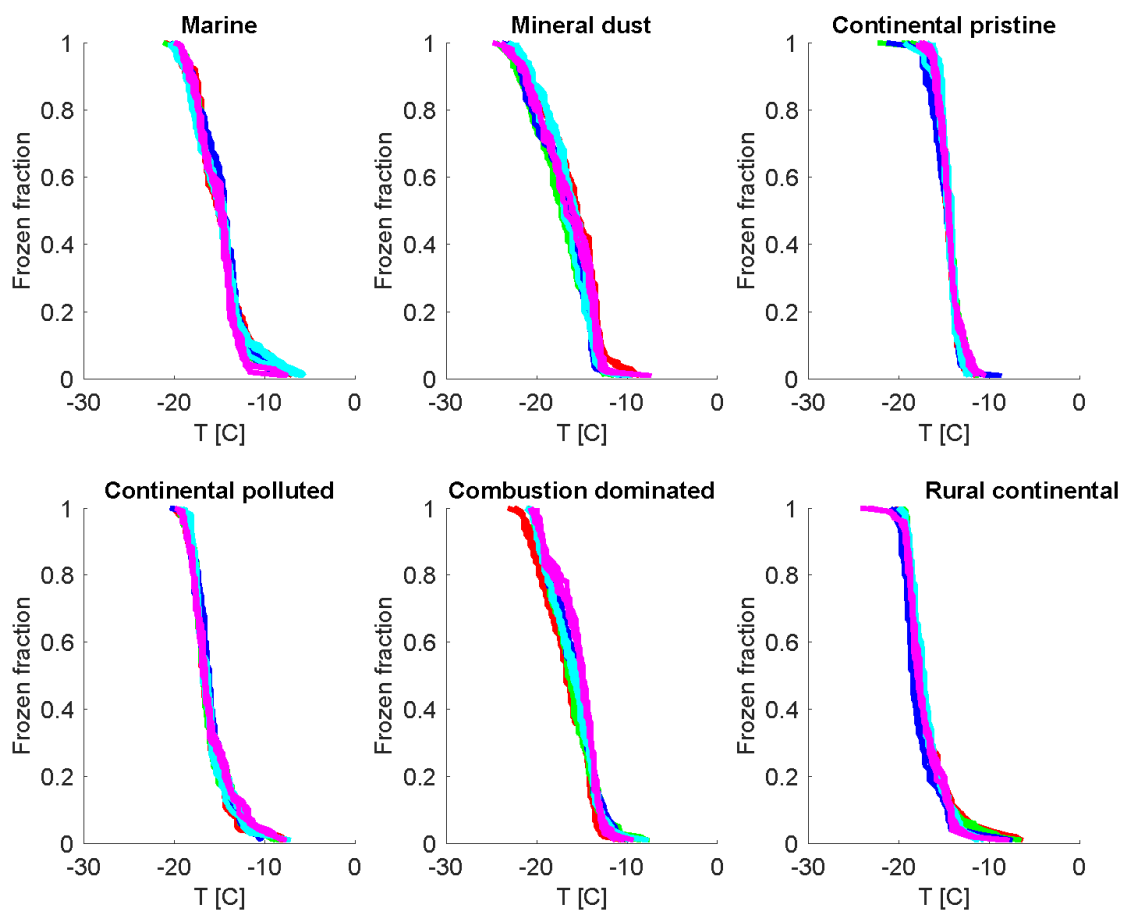
Figure 6: Freezing fraction as a function of cold-stage temperature for the 6 samples measured at constant cooling rate (2 K/min), (6 panels: Marine, Mineral dust influenced, Continental pristine, Continental polluted, Combustion dominated and rural continental samples). Each colour represents one of five different drop populations from any given sample exposed to the same cooling cycle starting at -5°C. For each drop population, at least 4 curves of the same colour are shown, each representing experiments at different times before, between and after the isothermal periods (2 -16 hours) regarding each panel. The time resolution of the imagery was 5 s which limits the accuracy of the determination of the freezing temperature (±0.1K).
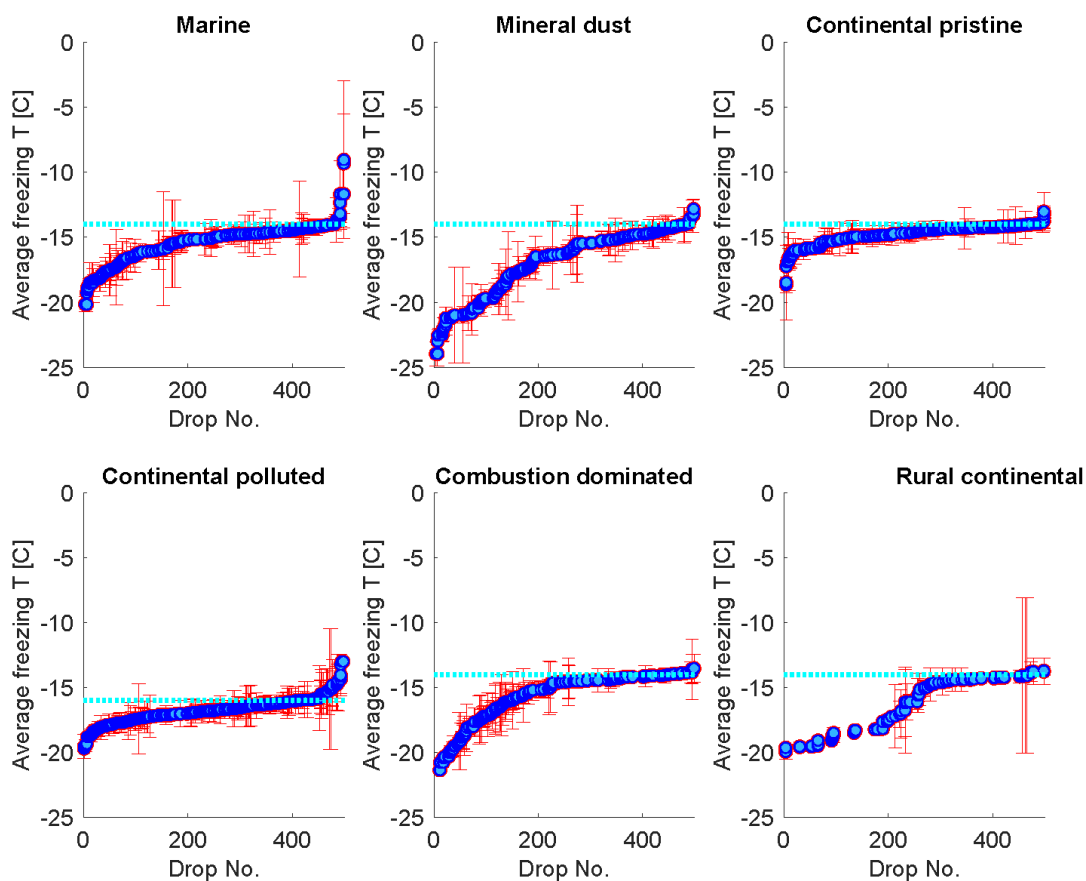
Figure 7: The average freezing temperature of each individual drop, and standard deviation, measured during the same constant cooling rate experiments depicted in Fig. 5 (minimum of 4 cooling cycles), for the marine dominated, mineral dust influenced,

885   continental pristine, continental polluted, combustion dominated and rural continental samples of aerosol material (panels from top left to lower right). All drops displayed also froze during the isothermal experiments (up to 10 hours). The temperature for the isothermal experiments is marked in each panel (cyan dotted line). The median value of the standard deviation for the normal freezing temperature of the individual drops were in the range between 0.25-0.34K.

890
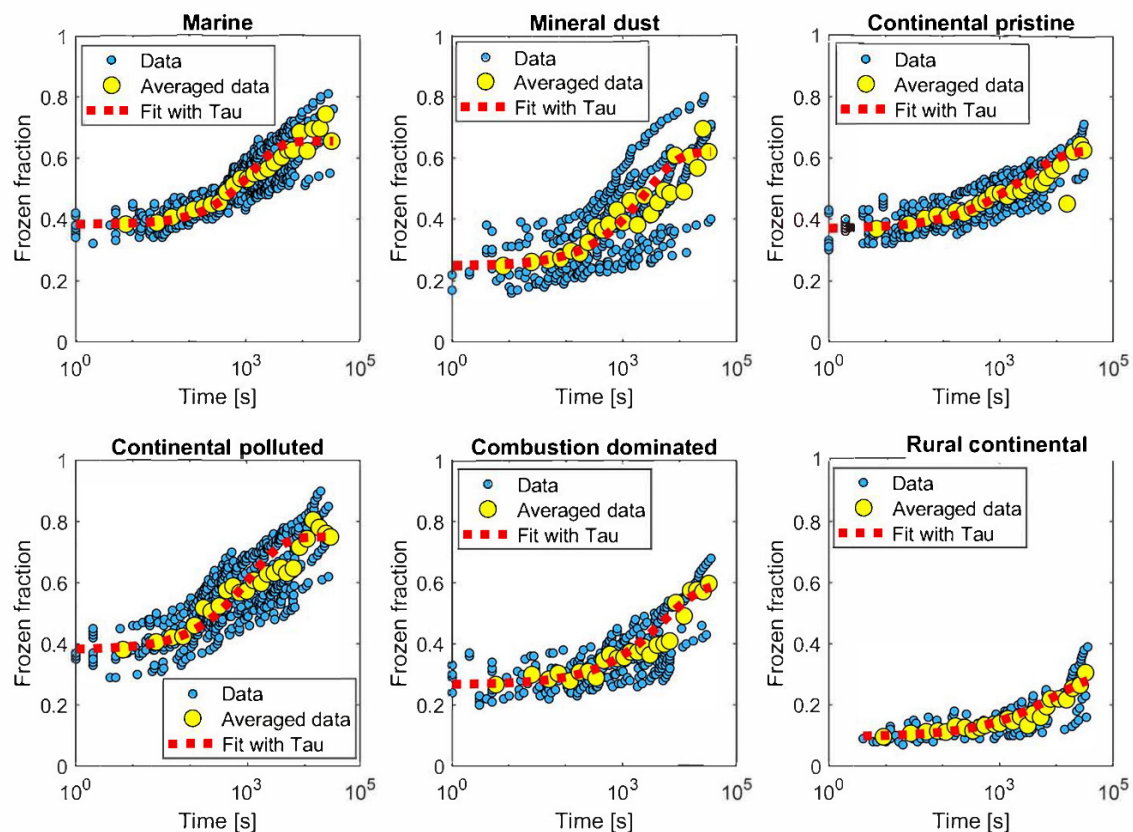
Figure 8: The measured freezing fractions as a function of time for the isothermal experiments (blue dots), which is averaged (yellow dots), for the marine dominated, mineral dust influenced, continental pristine, continental polluted, combustion dominated and rural continental samples of aerosol material (panels from top left to lower right). Also shown are the empirical fits using Eq (1) and the empirically determined relaxation time ($\tau(t)$) from the fits (Eq (3)) for the averaged data for the samples (red line).
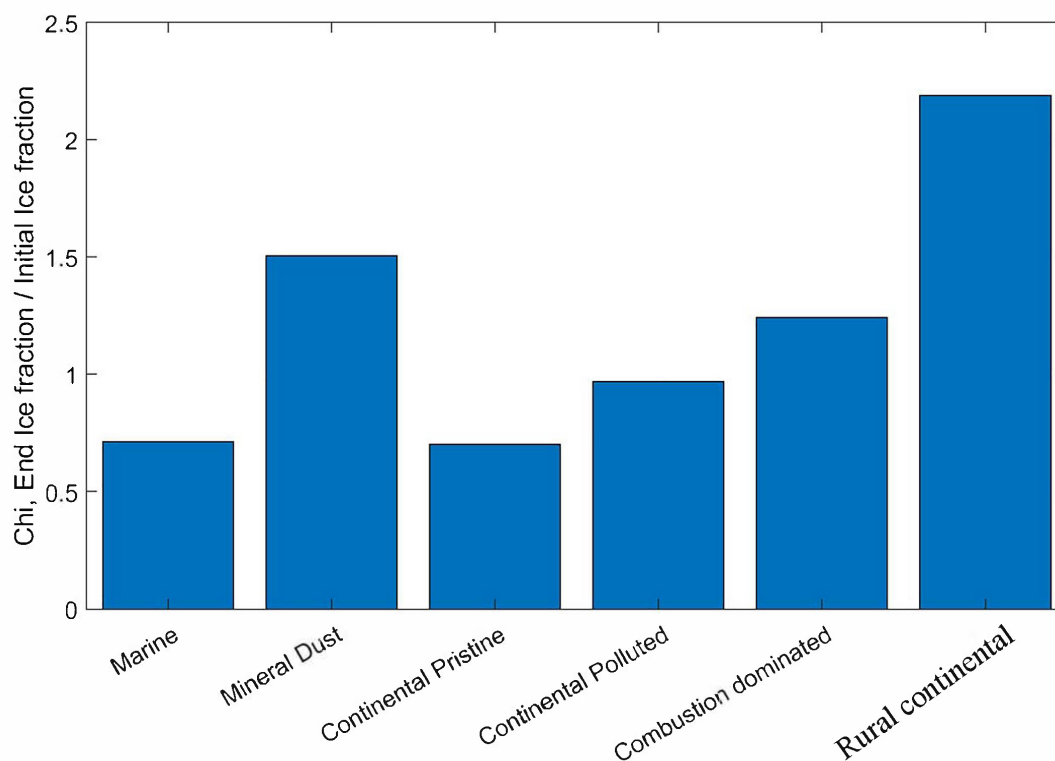
900 **Figure 9:** Fractional increase during 10 hours of the isothermal experiment in freezing fraction averaged as in Fig. 7 (initial and final yellow points), for the marine dominated, mineral dust influenced, continental pristine, continental polluted, combustion dominated and rural continental samples of aerosol material (left to right).
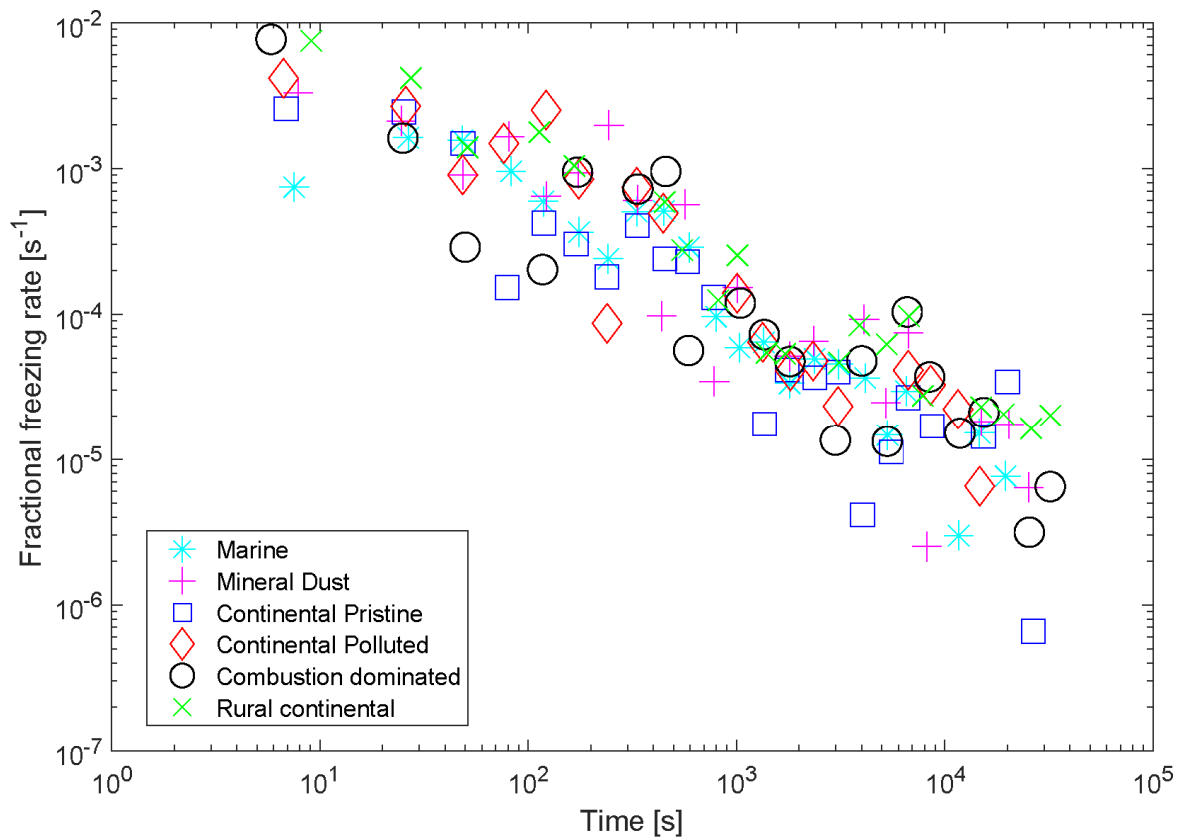
905

Figure 10: Fractional freezing rate ((1/N) (dN/dt)) plotted as a function of time since the start of the isothermal phase for the marine dominated, mineral dust influenced, continental pristine, continental polluted, combustion dominated and rural continental samples. Occasional negative rates are not plotted.
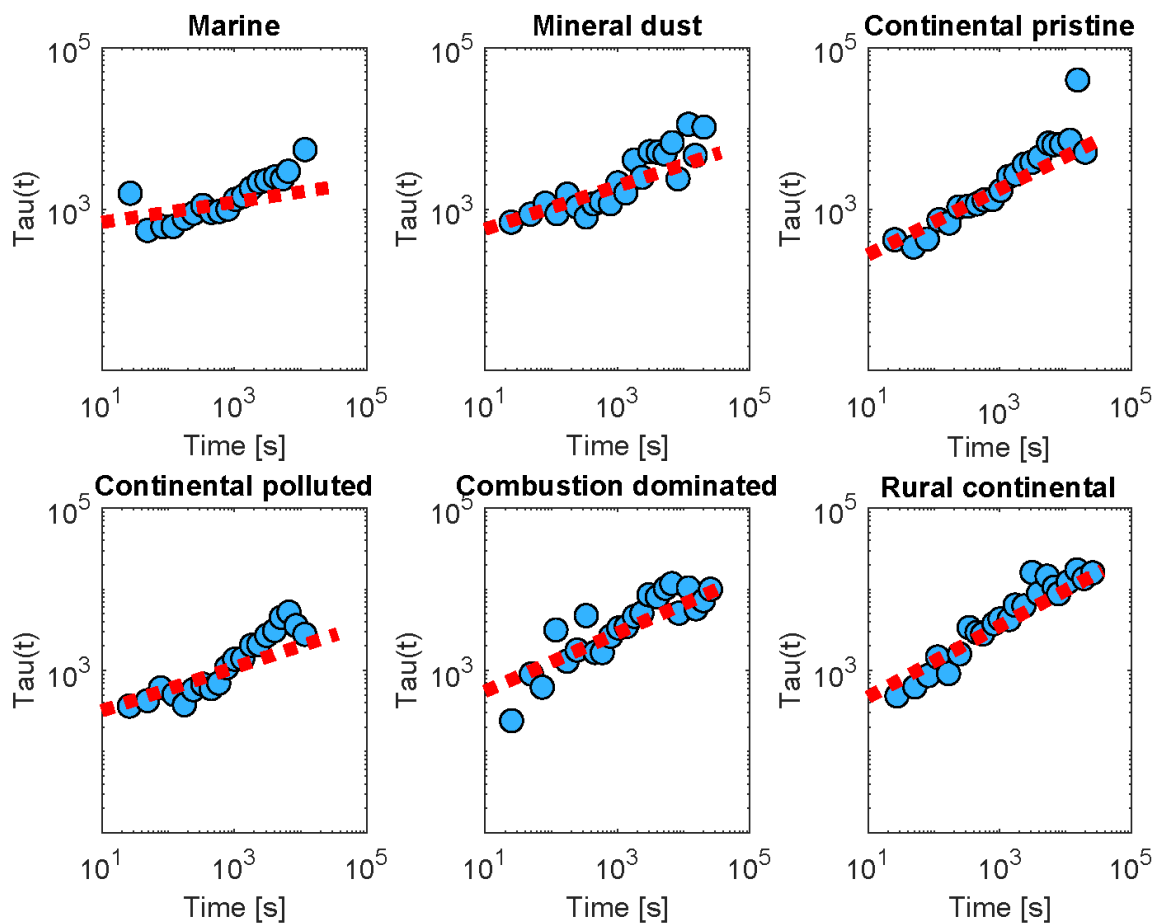
Figure 11: The relaxation time τ inferred from the isothermal experiments (up to 10 hours) using the averaged data (yellow dots in Figure 8), with Eq (2) as a function of time since the start of the isothermal phase (blue dots) for the marine dominated, mineral dust influenced, continental pristine, continental polluted, combustion dominated and rural continental samples of aerosol material (panels from top left to lower right). Also shown are empirical fits for all measurements of each sample using Eq (3), (red dotted line).
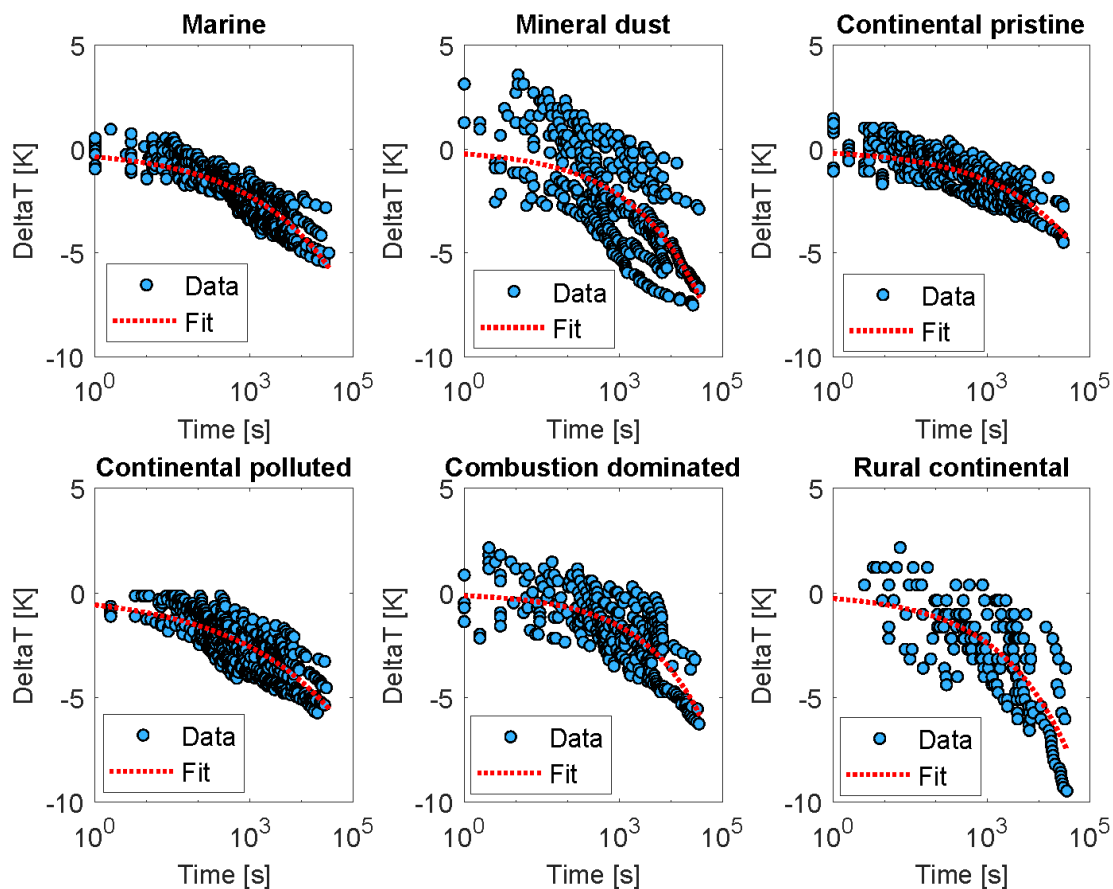
Figure 12: The apparent temperature shift, ΔT, required to match the empirical parameterization of the IN activity (Phillips *et al.* 2013) with the measurements of frozen fraction from the isothermal experiments (blue dots), for the marine dominated, mineral dust influenced, continental pristine, continental polluted, combustion dominated and rural continental samples of aerosol material (panels from top left to lower right). Evolution over time since the start of the isothermal phase is displayed. Also shown is the fit (Eq (5)) assuming a power law dependent on time (red dotted line).

920

925
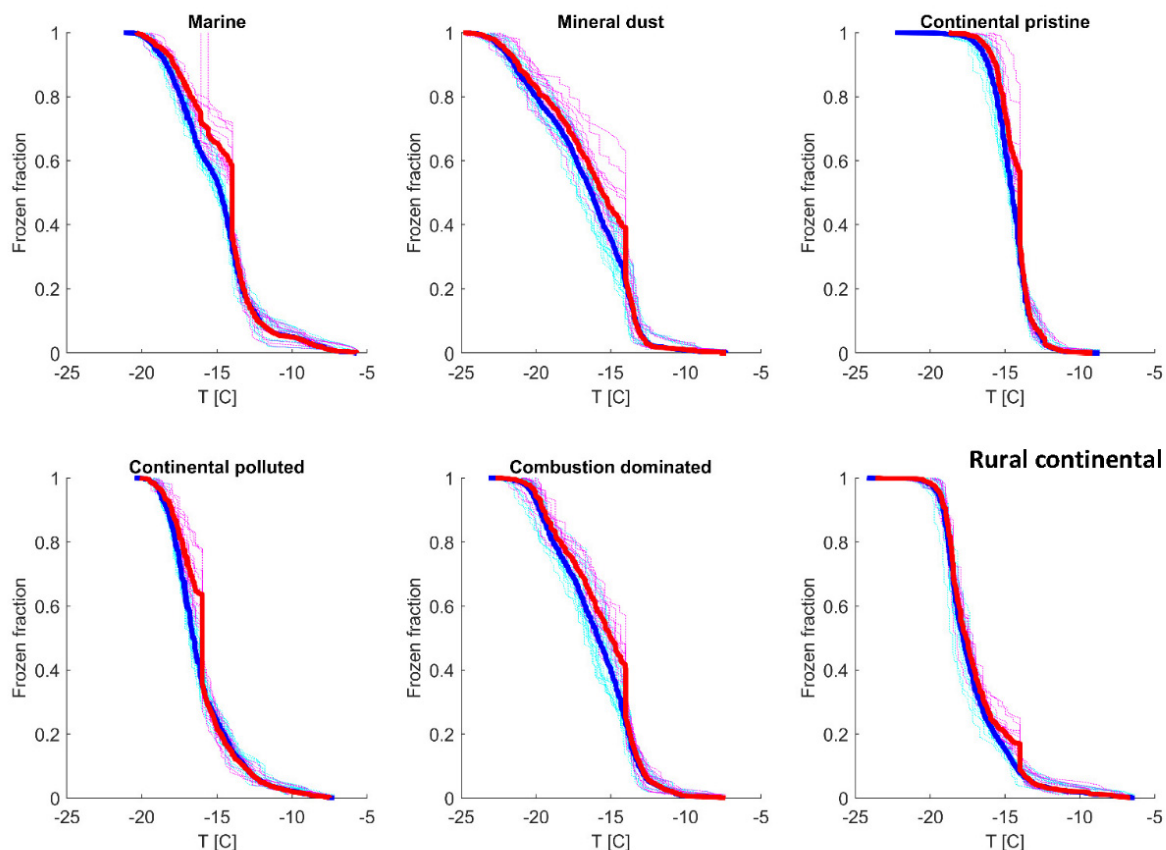
Figure 13: Frozen fraction raw data for the constant cooling rate experiments (cyan dotted lines) and for isothermal experiments of 2 hours (magenta dotted lines) for the marine dominated, mineral dust influenced, continental pristine, continental polluted, combustion dominated and rural continental samples of aerosol material (panels from top left to lower right). The large steps for two isothermal experiments displayed for the marine sample is an effect of a camera lag, not a physical effect, as they occur after the isothermal phase this does not influence the result. The averaged data for constant cooling rate experiments (blue lines) and isothermal experiments (red lines) are also shown. The offset seen for the isothermal experiments at the isothermal temperature is the effect of the 2-hour isothermal phase of the experiment. As seen in the figure, the samples behave almost identically until the isothermal phase is reached, and the isothermal data approaches the constant cooling rate data after the isothermal phase has elapsed, and constant cooling is resumed.

935 **Tables**

Table 1. Aerosol particle properties for the six studied samples during the respective sampling periods. The black carbon (BC) concentrations were inferred from the aethalometer at Hyltemossa. The concentrations of particulate matter (PM) were measured at the nearby Hallahus station. Data from February 2021 were not available due to instrument malfunctioning.

940

Sample type	Date	Sampling Duration [hours]	Median BC* [μg/m³]	Median PM$_1$ [μg/m³]	Median PM$_{10}$ [μg/m³]	PM$_{10}$-PM$_1$ [μg/m³]	
Marine	2020-09-05	16.8	0.054	2.29	9.24	7.1	945
Cont. Pristine	2020-11-29	24.0	0.044	1.71	3.41	1.6	
Cont. Polluted	2020-03-26	23.3	0.42	16.5	24.3	7.8	
Combustion	2020-12-07	6.5	0.43	17.9	20.85	3.0	
Rural continental	2020-09-18	18.4	0.051	0.85	5.84	4.7	
Mineral Dust	2021-02-23	6.1					950

955

Table 2: Empirically fitted parameters for Eq (3), $\hat{\tau}(t) = C_i t^\alpha$, with 95 % confidence bounds for the fitting parameters.

Sample type	C_i Fit	95% conf. bound lower	upper	α Fit	95% conf. bound lower	upper
Marine	515	231	1152	0.125	0.018	0.296 960
Mineral dust influenced	307	107	875	0.266	0.126	0.406
Continental pristine	107	32	362	0.406	0.243	0.568
Continental polluted	173	67	445.5	0.266	0.140	0.392
Combustion dominated	243	81	734	0.358	0.211	0.505
Rural continental	172	57	521	0.438	0.290	0.585 965

970

Table 3: Empirically fitted parameters of Eq (5), $\Delta T(t) = -A_i t^\beta$, with 95% confidence bounds for the fitting parameters.

Sample type	A_i Fit	*95% conf. bound*		*β*	*95% conf. bound*	
		lower	upper	Fit	lower	upper
Marine	0.376	0.328	0.425	0.261	0.245	0.277
Mineral dust influenced	0.240	0.148	0.332	0.323	0.280	0.367
Continental pristine	0.210	0.165	0.254	0.288	0.262	0.314
Continental polluted	0.575	0.502	0.648	0.217	0.201	0.233
Combustion dominated	0.131	0.082	0.180	0.362	0.320	0.405
Rural continental	0.267	0.147	0.386	0.319	0.269	0.368

975

980   **Table 4:** The averaged initial ice fractions for the samples at t = 0, and the observed average increase in ice fraction after 2- and 10-hours isothermal time. It should be noted that the experimental data for the isothermal time between 2 and 10 hours of exposure to constant conditions is much more limited than the data for the first 2 hours. This can also be seen in Figure 8. χ is the fractional increase in freezing fraction (FF) after 10 hours, also shown in Figure 9.

Sample type	Initial FF	Change in FF (2 hours)	Change in FF (10 hours)	χ
Marine	0.38	0.25	0.27	0.71
Mineral dust influenced	0.25	0.23	0.37	1.50
Continental pristine	0.37	0.15	0.26	0.70
Continental polluted	0.38	0.25	0.37	0.97
Combustion dominated	0.27	0.11	0.33	1.24
Rural continental	0.096	0.097	0.21	2.19